HIGH-ORDER ENERGY STABLE NUMERICAL SCHEMES FOR A NONLINEAR VARIATIONAL WAVE EQUATION MODELING NEMATIC LIQUID CRYSTALS IN TWO DIMENSIONS

PEDER AURSAND AND UJJWAL KOLEY

ABSTRACT. We consider a nonlinear variational wave equation that models the dynamics of the director field in nematic liquid crystals with high molecular rotational inertia. Being derived from an energy principle, energy stability is an intrinsic property of solutions to this model. For the two-dimensional case, we design numerical schemes based on the discontinuous Galerkin framework that either conserve or dissipate a discrete version of the energy.

Extensive numerical experiments are performed verifying the scheme's energy stability, order of convergence and computational efficiency. The numerical solutions are compared to those of a simpler first-order Hamiltonian scheme. We provide numerical evidence that solutions of the 2D variational wave equation loose regularity in finite time. After that occurs, dissipative and conservative schemes appear to converge to different solutions.

1. INTRODUCTION

1.1. **The Equation.** Liquid crystals (LCs) are mesophases, i.e., intermediate states of matter between the liquid and the crystal phase. They possess some of the properties of liquids (e.g. formation, fluidity) as well as some crystalline properties (e.g. electrical, magnetic, etc.) normally associated with solids. The nematic phase is the simplest of the liquid crystal mesophases, and is close to the liquid phase. It is characterized by long-range orientational order, i.e., the long axes of the molecules tend to align along a preferred direction, which can be considered invariant under rotation by an angle of π. The state of a nematic liquid crystals is usually given by two linearly independent vector fields; one describing the fluid flow and the other describing the dynamics of the preferred axis, which is defined by a vector $\mathbf{n}$ giving its local orientation. Under the assumption of constant degree of orientation, the magnitude of the *director field* $\mathbf{n}$ is usually taken to be unity. In the present work we focus exclusively on the dynamics of the director field (independently of any coupling with the fluid flow), a map

$$\mathbf{n} : \mathbb{R}^3 \times [0, \infty) \to \mathbb{S}^2$$

from the Euclidean space to the unit ball.

We consider the elastic dynamics of the liquid crystal director field in the inertia-dominated case (zero viscosity). Associated with the director field $\mathbf{n}$, the classical Oseen-Frank elastic energy density $\mathcal{W}$ is given by

$$\mathcal{W}(\mathbf{n}, \nabla\mathbf{n}) = \alpha \left| \mathbf{n} \times (\nabla \times \mathbf{n}) \right|^2 + \beta \left(\nabla \cdot \mathbf{n} \right)^2 + \gamma \left(\mathbf{n} \cdot (\nabla \times \mathbf{n}) \right)^2. \tag{1.1}$$

The constants α, β and γ are elastic material constants of the liquid crystal, and are associated with the three basic types of deformations of the medium; bend, splay and twist; respectively. Each of these constants must be positive in order to guarantee the existence of the minimum configuration of the energy $\mathcal{W}$ in the undistorted nematic configuration.

The one constant approximation ($\alpha = \beta = \gamma$) often provides a valuable tool to reach a qualitative insight into distortions of nematic configurations. Observe that, in this case the potential

energy density (1.1) reduces to the Dirichlet energy

$$\mathcal{W}(\mathbf{n}, \nabla\mathbf{n}) = \alpha \left|\nabla\mathbf{n}\right|^2.$$

This corresponds to the potential energy density used in harmonic maps into the sphere $\mathbb{S}^2$. The stability of the general Oseen–Frank potential energy equation, derived from the potential (1.1) using a variational principle, is studied by Ericksen and Kinderlehrer [8]. For the parabolic flow associated to (1.1), see [3, 7] and references therein.

In the regime in which inertial effects dominate viscosity, the dynamics of the director $\mathbf{n}$ is governed by the least action principle

$$\mathbb{J}(\mathbf{n}) = \iint \left(\mathbf{n}_t^2 - \mathcal{W}(\mathbf{n}, \nabla\mathbf{n})\right) dx\, dt, \qquad \mathbf{n} \cdot \mathbf{n} = 1. \tag{1.2}$$

Standard calculations reveal that the *Euler-Lagrange* equation associated to $\mathbb{J}$ is given by

$$\mathbf{n}_{tt} = \mathrm{div}\left(\mathcal{W}_{\nabla\mathbf{n}}(\mathbf{n}, \nabla\mathbf{n})\right) - \mathcal{W}_{\mathbf{n}}(\mathbf{n}, \nabla\mathbf{n}), \tag{1.3}$$

and is termed the variational wave equation. Introducing the *energy* and *energy density*

$$\mathcal{E}(t) = \int \left(\mathbf{n}_t^2 + \mathcal{W}(\mathbf{n}, \nabla\mathbf{n})\right) dx, \qquad \mathbf{E}(t, x) = \mathbf{n}_t^2 + \mathcal{W}(\mathbf{n}, \nabla\mathbf{n}),$$

it is easy to check the identities

$$\mathcal{E}' = 0, \qquad \mathbf{E}_t = \mathrm{div}\left(\mathcal{W}_{\nabla\mathbf{n}}(\mathbf{n}, \nabla\mathbf{n})\mathbf{n}_t\right),$$

in light of (1.3). Given the formidable difficulties in the mathematical analysis of (1.3), it is customary to investigate the particular case of a planar director field configuration.

The physical implications of considering the inertia-dominated regime warrants a comment. Indeed, in many experimental situations the inertial forces acting on the director are orders of magnitude smaller than the dissipative. For this reason, the inertial term is often neglected in modelling [25, 26, 9]. It was however noted early by Leslie [21] that inertial forces might be significant in cases where the director field is subjected to large accelerations. In general, inertia will be more significant in the small time-scale dynamics of the director. For this reason, their inclusion can be warranted in, e.g., liquid crystal acoustics [19], mechanical vibrations [27] and in cases with and external oscillating magnetic field [28].

1.1.1. *One-dimensional planar waves.* Planar deformations are central in the mathematical study of models for nematic liquid crystals. A simple such model can be derived by assuming that the deformation depends on a single space variable x and that the director field $\mathbf{n}$ in confined to the x-y plane. In this case we can write the director as

$$\mathbf{n} = (\cos u(x, t), \sin u(x, t), 0).$$

Geometrically, the molecules are lined up vertically on the x-y plane, and at each column (located at x) $u(x, t)$ measures the angle of the director field to the x-direction. With the above simplifications, the variational principle (1.2) reduces to

$$\begin{cases} u_{tt} - c(u)\left(c(u)u_x\right)_x = 0, & (x, t) \in \Pi_T, \\ u(x, 0) = u_0(x), & x \in \mathbb{R}, \\ u_t(x, 0) = u_1(x), & x \in \mathbb{R}, \end{cases} \tag{1.4}$$

where $\Pi_T = \mathbb{R} \times [0, T]$ with fixed $T > 0$, and the wave speed $c(u)$ given by

$$c^2(u) = \alpha \cos^2 u + \beta \sin^2 u. \tag{1.5}$$

Initially considered by Hunter and Saxton [23, 17], (1.4) is the simplest form of the nonlinear variational wave equation (1.3) studied in the literature.

1.1.2. *Two-dimensional planar waves.* Planar deformations can also be studied in two dimensions. Specifically, if we assume that the deformation depends on two space variables x, y, the director can be written in the form

$$\mathbf{n} = (\cos u(x, y, t),\ \sin u(x, y, t),\ 0)$$

with u being the angle to the x-z plane. The corresponding variational wave equation is given by

$$\begin{cases} u_{tt} - c(u)\,(c(u)u_x)_x - b(u)\,(b(u)u_y)_y - a'(u)u_x u_y - 2a(u)u_{xy} = 0, & (x, y, t) \in \mathbb{Q}_T, \\ u(x, y, 0) = u_0(x, y), & (x, y) \in \mathbb{R}^2, \\ u_t(x, y, 0) = u_1(x, y), & (x, y) \in \mathbb{R}^2, \end{cases} \tag{1.6}$$

where $\mathbb{Q}_T = \mathbb{R}^2 \times [0, T]$ with $T > 0$ fixed, $u : \mathbb{Q}_T \to \mathbb{R}$ is the unknown function and a, b, c are given by

$$c^2(u) = \alpha \cos^2 u + \beta \sin^2 u,$$
$$b^2(u) = \alpha \sin^2 u + \beta \cos^2 u,$$
$$a(u) = \frac{\alpha - \beta}{2} \sin(2u).$$

In this picture, $c(u)$ is the wave speed in the x-direction and $b(u)$ is the wave speed in the y-direction.

For smooth solutions of (1.6) it is straightforward to verify that the energy

$$\begin{aligned} \mathcal{E}(t) &= \iint_{\mathbb{R}^2} \left(u_t^2 + c^2(u)u_x^2 + b^2(u)u_y^2 + 2a(u)u_x u_y \right) dx\, dy \\ &= \iint_{\mathbb{R}^2} u_t^2 + (\alpha(\cos(u)u_x + \sin(u)u_y))^2 + (\beta(\sin(u)u_x - \cos(u)u_y))^2\ dx\, dy \end{aligned} \tag{1.7}$$

is conserved, i.e., we have

$$\frac{d\mathcal{E}(t)}{dt} \equiv 0. \tag{1.8}$$

Moreover, for all $t \in [0, T]$ we have

$$\iint_{\mathbb{R}^2} \left(u_t^2 + \min\{\alpha, \beta\}(u_x^2 + u_y^2) \right) dx\, dy \leq \mathcal{E}(t) \leq \iint_{\mathbb{R}^2} \left(u_t^2 + \max\{\alpha, \beta\}(u_x^2 + u_y^2) \right) dx\, dy.$$

In particular, it follows that $\mathcal{E}(t) \geq 0$ for all $t \in [0, T]$. To see this, first we consider $\alpha \geq \beta$ (for $\alpha \leq \beta$, we argue in the same way). Then

$$\begin{aligned} c^2(u)&u_x^2 + b^2(u)u_y^2 + 2a(u)u_x u_y \\ &= \left(\alpha \cos^2(u) + \beta \sin^2(u) \right) u_x^2 + \left(\alpha \sin^2 u + \beta \cos^2 u \right) u_y^2 + 2(\alpha - \beta) \sin(u) \cos(u)u_x u_y \\ &\leq \left(\alpha \cos^2(u) + \beta \sin^2(u) \right) u_x^2 + \left(\alpha \sin^2 u + \beta \cos^2 u \right) u_y^2 + 2(\alpha - \beta) |\sin(u) \cos(u)u_x u_y| \\ &= \alpha \left(\cos^2(u)u_x^2 + \sin^2(u)u_y^2 + 2 |\sin(u) \cos(u)u_x u_y| \right) \\ &\quad + \beta \left(\sin^2(u)u_x^2 + \cos^2(u)u_y^2 - 2 |\sin(u) \cos(u)u_x u_y| \right) \\ &= \alpha \left(|\cos(u)u_x| + |\sin(u)u_y| \right)^2 + \beta \left(|\sin(u)u_x| - |\cos(u)u_y| \right)^2 \\ &\leq \alpha \left[\left(|\cos(u)u_x| + |\sin(u)u_y| \right)^2 + \left(|\sin(u)u_x| - |\cos(u)u_y| \right)^2 \right] = \alpha(u_x^2 + u_y^2), \end{aligned}$$

and

$$\begin{aligned} c^2(u)&u_x^2 + b^2(u)u_y^2 + 2a(u)u_x u_y \\ &= \left(\alpha \cos^2(u) + \beta \sin^2(u) \right) u_x^2 + \left(\alpha \sin^2 u + \beta \cos^2 u \right) u_y^2 + 2(\alpha - \beta) \sin(u) \cos(u)u_x u_y \\ &\geq \left(\alpha \cos^2(u) + \beta \sin^2(u) \right) u_x^2 + \left(\alpha \sin^2 u + \beta \cos^2 u \right) u_y^2 - 2(\alpha - \beta) |\sin(u) \cos(u)u_x u_y| \\ &= \alpha \left(\cos^2(u)u_x^2 + \sin^2(u)u_y^2 - 2 |\sin(u) \cos(u)u_x u_y| \right) \\ &\quad + \beta \left(\sin^2(u)u_x^2 + \cos^2(u)u_y^2 + 2 |\sin(u) \cos(u)u_x u_y| \right) \\ &= \alpha \left(|\cos(u)u_x| - |\sin(u)u_y| \right)^2 + \beta \left(|\sin(u)u_x| + |\cos(u)u_y| \right)^2 \end{aligned}$$

$$\geq \beta \Big[\left(|\cos(u)u_x| - |\sin(u)u_y| \right)^2 + \left(|\sin(u)u_x| + |\cos(u)u_y| \right)^2 \Big] = \beta(u_x^2 + u_y^2).$$

1.2. **Mathematical Difficulties.** There exists a fairly satisfactory well posedness theory for the one dimensional equation (1.4). However, despite its apparent simplicity, the mathematical analysis of (1.4) is complicated. Independently of the smoothness of the initial data, due to the nonlinear nature of the equation, singularities may form in the solution [10, 12, 11]. Therefore, solutions of (1.4) should be interpreted in the weak sense:

Definition 1.1. *Set* $\Pi_T = \mathbb{R} \times (0, T)$. *A function*

$$u(t, x) \in L^\infty\left([0, T]; W^{1,p}(\mathbb{R})\right) \cap C(\Pi_T), u_t \in L^\infty\left([0, T]; L^p(\mathbb{R})\right),$$

for all $p \in [1, 3 + q]$, *where* q *is some positive constant, is a weak solution of the initial value problem* (1.4) *if it satisfies:*

*(**D.1**) For all test functions* $\varphi \in \mathcal{D}(\mathbb{R} \times [0, T))$

$$\iint_{\Pi_T} \left(u_t \varphi_t - c^2(u)u_x \varphi_x - c(u)c'(u)(u_x)^2 \varphi \right) \, dx \, dt = 0. \tag{1.9}$$

*(**D.2**)* $u(\cdot, t) \to u_0$ *in* $C\left([0, T]; L^2(\mathbb{R})\right)$ *as* $t \to 0^+$.
*(**D.3**)* $u_t(\cdot, t) \to u_1$ *as a distribution in* Π_T *when* $t \to 0^+$.

In recent years, there has been an increased interest to understand the different classes of weak solutions (conservative and dissipative) of the Cauchy problem (1.4), under the restrictive assumption on the wave speed c (positivity of the derivative of c). The literature herein is substantial, and we will here only give a non-exhaustive overview. Within the existing framework, we mention the papers by Zhang and Zheng [29, 30, 31, 32, 33, 34], Bressan and Zheng [4] and Holden and Raynaud [15]. In fact, taking advantage of Young measure theory, existence of a global weak solution with initial data $u_0 \in H^1(\mathbb{R})$ and $u_1 \in L^2(\mathbb{R})$ has been proved in [33]. However, the regularity assumptions on the wave speed $c(u)$ ($c(u)$ is smooth, bounded, positive with derivative that is non-negative and strictly positive on the initial data u_0) in the analysis of [29, 30, 31, 32, 33, 34] precludes consideration of the physical wave speed given by (1.5).

A novel approach to the study of (1.4) was taken by Bressan and Zheng [4]. They have constructed the solutions by introducing new variables related to the characteristics, leading to a characterization of singularities in the energy density. The solution u, constructed by the above principle, is locally Lipschitz continuous and the map $t \to u(t, \cdot)$ is continuously differentiable with values in $L^p_{\text{loc}}(\mathbb{R})$ for $1 \leq p < 2$.

Drawing preliminary motivation from [4], Holden and Raynaud [15] provides a rigorous construction of a semigroup of conservative solutions of (1.4). Since their construction is based on energy measures as independent variables, the formation of singularities is somewhat natural and they were able to overcome the non-physical condition on wave speed ($c'(u) > 0$). Moreover, their analysis can incorporate initial data u_0, u_1 that contain measures.

On the other side, the existence of solutions to two dimensional planar waves (1.6) is completely open. Contrary to its one dimensional counterpart, it is not possible to rewrite (1.6) as a system of equations in terms of Riemann invariants (for a brief justification, see Sec 2). Therefore, the same proofs do not apply mutatis mutandis in the two dimensional case. Having said this, one can of course rewrite (1.6) as a first order system using different change of variables (see Sec 2). However, due to lack of "symmetry" of this formulation, it is hard to establish well posedness of such equations using this approach.

1.3. **Numerical Schemes.** Except under very simplifying assumptions, there does not exist elementary and explicit solutions for (1.4). Moreover, the existence of two classes of weak solutions renders the initial value problem ill-posed after the formation of singularities. Consequently, robust numerical schemes are important in the study of the variational wave equation. Furthermore, capturing conservative solutions numerically is indeed a delicate issue since we expect that traditional finite difference schemes will not yield conservative solutions, due to the intrinsic numerical diffusion in these schemes.

There is a sparsity of efficient numerical schemes for the 1D equation (1.4) available in the literature. We can refer to [11], where the authors present some numerical examples to illustrate their theory. By the way of the theory of Young's measure-valued solutions, Holden et. al. [16] proved convergence of the numerical approximation generated by a semi-discrete finite difference scheme for one-dimensional equation (1.4) to the *dissipative* weak solution of (1.4), under a restrictive assumption on the wave speed ($c'(u) > 0$). To overcome such non-physical assumptions, Holden and Raynaud [15] used their analytical construction, as mentioned earlier, to define a numerical method that can approximate the *conservative* solution. However, the main drawback of this method is that it is computationally very expensive as there is no time marching.

Finally, we mention recent papers [20, 1] which deals with finite difference schemes and discontinuous Galerkin schemes, respectively, for (1.4). Their main idea was to rewrite (1.4) in the form of a first order systems and design numerical schemes for those systems. The key design principle was either energy conservation or energy dissipation. In that context, they have presented schemes that either conserve or dissipate the discrete energy. They also validated the properties of the schemes via extensive numerical experiments.

Numerical results for the two-dimensional variational wave equation (1.6) are even more sparse than for the one-dimensional case. In fact, to the best of the authors' knowledge, the only available numerical experiments are given in the final section of the recent paper by Koley et al. [20].

1.4. **Scope and Outline of the Paper.** The purpose of this paper is to develop efficient high-order schemes for the two-dimensional nonlinear variational wave equation (1.6). By using the Runge–Kutta Discontinuous Galerkin (RK-DG) framework we aim to derive schemes that either *conserve* or *dissipate* a discrete version of the energy inherited from the variational formulation of the problem. Since the behavior of solutions to the 2D equation (1.6) is largely unknown, these schemes will allow us to begin investigate if crucial properties of the 1D equation (1.4) carry over in the two-dimensional case. To the best of our knowledge, this is the first systematic numerical study of the two-dimensional variational wave equation (1.6).

Our approach for constructing high-order schemes is the RK-DG method [13, 6], where the test and trial functions are discontinuous piecewise polynomials. In contrast to high order finite-volume schemes, the high order of accuracy is already built into the finite dimensional spaces and no reconstruction is needed. Exact or approximate Riemann solvers from finite volume methods are used to compute the numerical fluxes between elements. For an energy dissipative scheme we will employ a combination of dissipative fluxes and, in order to control possible spurious oscillations near shocks, shock capturing operators [18, 5, 2]. These methods have recently been shown to be entropy stable for conservation laws [14]. In contrast to for finite volume methods, entropy stability has gained more attention in finite element methods since one advantage of this method is that the formulation immediately allows the use of general unstructured grids.

The shock capturing DG schemes in this paper have the following properties:

(1) The schemes are arbitrarily high-order accurate.
(2) The schemes are robust and resolved the solution (including possible singularities in the angle u) in a stable manner.
(3) The energy conservative scheme preserve the discrete energy at the semi-discrete level. Using a high-order time stepping method, this property also holds in the fully discrete case for all orders of accuracy tested.
(4) The energy dissipative scheme dissipate the discrete energy at the semi-discrete level. Using a high-order time stepping method, this property also holds in the fully discrete case for all orders of accuracy tested.

In the current presentation we consider, for simplicity, a Cartesian grid. The schemes can however be generalized to more general geometries. For such applications, it might be useful to write (1.6) in the form

$$u_{tt} - (T(u)\nabla)(T(u)\nabla u) = 0 \tag{1.10}$$

where

$$T(u) = \begin{pmatrix} \sqrt{\alpha}\cos(u) & \sqrt{\alpha}\sin(u) \\ -\sqrt{\beta}\sin(u) & \sqrt{\beta}\cos(u) \end{pmatrix}.$$

The rest of the paper is organized as follows: In Section 2, we present energy conservative and energy dissipative schemes for the one-dimensional equation (1.6). Section 3 concerns a first-order Hamiltonian (energy preserving) scheme for comparison. Section 4 contains numerical experiments verifying the order of convergence, energy stability and efficiency of the schemes.

2. Discontinuous Galerkin Schemes in Two-space Dimensions

Drawing primary motivation from the one-dimensional case [1], we aim to design energy conservative and energy dissipative discontinuous Galerkin schemes of the two-dimensional version of the nonlinear variational wave equation (1.6), by rewriting it as a first-order system. First, we briefly mention why formulation based on Riemann invariants does not work in two dimensional case.

2.1. **The system of equations.** We introduce three new independent variables:

$$p := u_t,$$
$$v := \cos(u)u_x + \sin(u)u_y,$$
$$w := \sin(u)u_x - \cos(u)u_y.$$

Then, for smooth solutions, we see that

$$v_t = \cos(u)u_{xt} - \sin(u)u_t u_x + \sin(u)u_{yt} + \cos(u)u_t u_y$$
$$= (\cos(u)u_t)_x - u_t(\cos(u))_x + (\sin(u)u_t)_y - u_t(\sin(u))_y - u_t\left(\sin(u)u_x - \cos(u)u_y\right),$$

and

$$w_t = \sin(u)u_{xt} + \cos(u)u_t u_x - \cos(u)u_{yt} + \sin(u)u_t u_y$$
$$= (\sin(u)u_t)_x - u_t(\sin(u))_x - (\cos(u)u_t)_y + u_t(\cos(u))_y + u_t\left(\cos(u)u_x + \sin(u)u_y\right).$$

Moreover, a straightforward calculation using equation (1.6) reveals that

$$p_t - (\alpha - \beta)\left(\cos(u)\sin(u)u_x^2 - \cos^2(u)u_x u_y + \sin^2(u)u_x u_y - \cos(u)\sin(u)u_y^2\right)$$
$$= \alpha\left(\cos(u)(\cos(u)u_x + \sin(u)u_y)\right)_x + \alpha\left(\sin(u)(\cos(u)u_x + \sin(u)u_y)\right)_y$$
$$+ \beta\left(\sin(u)(\sin(u)u_x - \cos(u)u_y)\right)_x - \beta\left(\cos(u)(\sin(u)u_x - \cos(u)u_y)\right)_y.$$

Hence, for smooth solutions, equation (1.6) is equivalent to the following system for (p, v, w, u),

$$\begin{cases} p_t - \alpha(f(u)v)_x - \alpha(g(u)v)_y - \beta(g(u)w)_x + \beta(f(u)w)_y - \alpha vw + \beta vw = 0, \\ v_t - (f(u)p)_x + pf(u)_x - (g(u)p)_y + pg(u)_y + pw = 0, \\ w_t - (g(u)p)_x + pg(u)_x + (f(u)p)_y - pf(u)_y - pv = 0, \\ u_t = p, \end{cases} \tag{2.1}$$

where $f(u) := \cos(u)$, and $g(u) := \sin(u)$. Furthermore, the corresponding energy associated with the system (2.1) is

$$\mathcal{E}(t) = \iint_{\mathbb{R}^2} \left(p^2 + \alpha v^2 + \beta w^2\right)\,\mathrm{d}x\,\mathrm{d}y. \tag{2.2}$$

A simple calculation shows that smooth solutions of (2.1) satisfy the energy identity:

$$\left(p^2 + \alpha v^2 + \beta w^2\right)_t + 2\left(\alpha p f(u)v + \beta p g(u)w\right)_x + 2\left(\alpha p g(u)v - \beta p f(u)w\right)_y = 0. \tag{2.3}$$

Hence, the fact that the total energy (2.2) is conserved follows from integrating the above identity in space and assuming that the functions p, u, v and w decay at infinity.

2.2. **The grid.** We begin by introducing some notation needed to define the DG schemes. Let the domain $\Omega \subset \mathbb{R}^2$ be decomposed as $\Omega = \cup_{i,j}\Omega_{ij}$ with $\Omega_{ij} := \Omega_i \times \Omega_j$ where $\Omega_i = [x_{i-1/2}, x_{i+1/2}]$ and $\Omega_j = [y_{j-1/2}, y_{j+1/2}]$ for $i, j = 1, \cdots, N$. Moreover, we denote $\Delta x_i = x_{i+1/2} - x_{i-1/2}$ and $\Delta y_j = y_{j+1/2} - y_{j-1/2}$. Furthermore, we also denote $x_i = (x_{i-1/2} + x_{i+1/2})/2$ and $y_j = (y_{j-1/2} + y_{j+1/2})/2$.

Let u be a grid function and denote $u^+_{i+1/2}(y)$ as the function evaluated at the right side of the cell interface at $x_{i+1/2}$ and let $u^-_{i+1/2}(y)$ denote the value at the left side. Similarly, we let $u^+_{j+1/2}(x)$ be the function evaluated at the upper side of the cell interface at $y_{i+1/2}$ and let $u^-_{j+1/2}(x)$ denote the value at the lower side. We can then introduce the jump and, respectively, the average of any grid function u across the interfaces as

$$\overline{u}_{i+1/2}(y) := \frac{u^+_{i+1/2}(y) + u^-_{i+1/2}(y)}{2}, \quad \overline{u}_{j+1/2}(x) := \frac{u^+_{j+1/2}(x) + u^-_{j+1/2}(x)}{2},$$

$$[\![u]\!]_{i+1/2}(y) := u^+_{i+1/2}(y) - u^-_{i+1/2}(y), \quad [\![u]\!]_{j+1/2}(x) := u^+_{j+1/2}(x) - u^-_{j+1/2}(x).$$

Moreover, let v be another grid function. Then the following identities are readily verified:

$$[\![uv]\!]_{i+1/2} = \overline{u}_{i+1/2}[\![v]\!]_{i+1/2} + [\![u]\!]_{i+1/2}\overline{v}_{i+1/2}, \quad [\![uv]\!]_{j+1/2} = \overline{u}_{j+1/2}[\![v]\!]_{j+1/2} + [\![u]\!]_{j+1/2}\overline{v}_{j+1/2} \tag{2.4}$$

2.3. **Variational Formulation.** We seek an approximation (p, v, w, u) of (2.1) such that for each $t \in [0, T]$, p, v, w, and u belong to finite dimensional space

$$X_h^s(\Omega) = \left\{u \in L^2(\Omega) : u|_{\Omega_{ij}} \text{ polynomial of degree} \leq p\right\}.$$

The variational form is derived by multiplying the strong form (2.1) with test functions $\phi, \nu, \psi, \zeta \in X_h^s(\Omega)$ and integrating over each element separately. After using integration-by-parts, we obtain

$$\sum_{i,j=1}^N \int_{\Omega_{ij}} p_t\,\phi\,\mathrm{d}x\,\mathrm{d}y + \alpha \sum_{i,j=1}^N \int_{\Omega_{ij}} f(u)\,v\,\phi_x\,\mathrm{d}x\,\mathrm{d}y - \alpha \sum_{i,j=1}^N \int_{\Omega_j} (fv)_{i+1/2}\,\phi^-_{i+1/2}\,\mathrm{d}y$$

$$+ \alpha \sum_{i,j=1}^N \int_{\Omega_j} (fv)_{i-1/2}\,\phi^+_{i-1/2}\,\mathrm{d}y + \alpha \sum_{i,j=1}^N \int_{\Omega_{ij}} g(u)\,v\,\phi_y\,\mathrm{d}x\,\mathrm{d}y - \alpha \sum_{i,j=1}^N \int_{\Omega_i} (gv)_{j+1/2}\,\phi^-_{j+1/2}\,\mathrm{d}x$$

$$+ \alpha \sum_{i,j=1}^N \int_{\Omega_i} (gv)_{j-1/2}\,\phi^+_{j-1/2}\,\mathrm{d}x + \beta \sum_{i,j=1}^N \int_{\Omega_{ij}} g(u)\,w\,\phi_x\,\mathrm{d}x\,\mathrm{d}y - \beta \sum_{i,j=1}^N \int_{\Omega_j} (gw)_{i+1/2}\,\phi^-_{i+1/2}\,\mathrm{d}y$$

$$+ \beta \sum_{i,j=1}^N \int_{\Omega_j} (gw)_{i-1/2}\,\phi^+_{i-1/2}\,\mathrm{d}y - \beta \sum_{i,j=1}^N \int_{\Omega_j} f(u)\,w\,\phi_y\,\mathrm{d}x\,\mathrm{d}y + \beta \sum_{i,j=1}^N \int_{\Omega_i} (fw)_{j+1/2}\,\phi^-_{j+1/2}\,\mathrm{d}x$$

$$- \beta \sum_{i,j=1}^N \int_{\Omega_i} (fw)_{j-1/2}\,\phi^+_{j-1/2}\,\mathrm{d}x - \alpha \sum_{i,j=1}^N \int_{\Omega_{ij}} v\,w\,\phi\,\mathrm{d}x\,\mathrm{d}y + \beta \sum_{i,j=1}^N \int_{\Omega_{ij}} v\,w\,\phi\,\mathrm{d}x\,\mathrm{d}y = 0, \tag{2.5}$$

and

$$\sum_{i,j=1}^N \int_{\Omega_{ij}} v_t\,\nu\,\mathrm{d}x\,\mathrm{d}y + \sum_{i,j=1}^N \int_{\Omega_{ij}} f(u)\,p\,\nu_x\,\mathrm{d}x\,\mathrm{d}y - \sum_{i,j=1}^N \int_{\Omega_j} (f\,p)_{i+1/2}\,\nu^-_{i+1/2}\,\mathrm{d}y$$

$$+ \sum_{i,j=1}^N \int_{\Omega_j} (f\,p)_{i-1/2}\,\nu^+_{i-1/2}\,\mathrm{d}y - \sum_{i,j=1}^N \int_{\Omega_{ij}} f(u)\,(p\,\nu)_x\,\mathrm{d}x\,\mathrm{d}y + \sum_{i,j=1}^N \int_{\Omega_j} (f)_{i+1/2}\,p^-_{i+1/2}\,\nu^-_{i+1/2}\,\mathrm{d}y$$

$$- \sum_{i,j=1}^N \int_{\Omega_j} (f)_{i-1/2}\,p^+_{i-1/2}\,\nu^+_{i-1/2}\,\mathrm{d}y + \sum_{i,j=1}^N \int_{\Omega_{ij}} g(u)\,p\,\nu_y\,\mathrm{d}x\,\mathrm{d}y - \sum_{i,j=1}^N \int_{\Omega_i} (g\,p)_{j+1/2}\,\nu^-_{j+1/2}\,\mathrm{d}x$$

$$+ \sum_{i,j=1}^N \int_{\Omega_i} (g\,p)_{j-1/2}\,\nu^+_{j-1/2}\,\mathrm{d}x - \sum_{i,j=1}^N \int_{\Omega_{ij}} g(u)\,(p\,\nu)_y\,\mathrm{d}x\,\mathrm{d}y + \sum_{i,j=1}^N \int_{\Omega_i} (g)_{j+1/2}\,p^-_{j+1/2}\,\nu^-_{j+1/2}\,\mathrm{d}x$$

$$- \sum_{i,j=1}^{N} \int_{\Omega_i} (g)_{j-1/2} \, p_{j-1/2}^{+} \, \nu_{j-1/2}^{+} \, \mathrm{d}x + \sum_{i,j=1}^{N} \int_{\Omega_{ij}} p \, w \, \nu \, \mathrm{d}x \, \mathrm{d}y = 0, \quad (2.6)$$

and

$$\sum_{i,j=1}^{N} \int_{\Omega_{ij}} w_t \, \psi \, \mathrm{d}x \, \mathrm{d}y + \sum_{i,j=1}^{N} \int_{\Omega_{ij}} g(u) \, p \, \psi_x \, \mathrm{d}x \, \mathrm{d}y - \sum_{i,j=1}^{N} \int_{\Omega_j} (g \, p)_{i+1/2} \, \psi_{i+1/2}^{-} \, \mathrm{d}y$$

$$+ \sum_{i,j=1}^{N} \int_{\Omega_j} (g \, p)_{i-1/2} \, \psi_{i-1/2}^{+} \, \mathrm{d}y - \sum_{i,j=1}^{N} \int_{\Omega_{ij}} g(u) \, (p \, \psi)_x \, \mathrm{d}x \, \mathrm{d}y + \sum_{i,j=1}^{N} \int_{\Omega_j} (g)_{i+1/2} \, p_{i+1/2}^{-} \, \psi_{i+1/2}^{-} \, \mathrm{d}y$$

$$- \sum_{i,j=1}^{N} \int_{\Omega_j} (g)_{i-1/2} \, p_{i-1/2}^{+} \, \psi_{i-1/2}^{+} \, \mathrm{d}y - \sum_{i,j=1}^{N} \int_{\Omega_{ij}} f(u) \, p \, \psi_y \, \mathrm{d}x \, \mathrm{d}y + \sum_{i,j=1}^{N} \int_{\Omega_i} (f \, p)_{j+1/2} \, \psi_{j+1/2}^{-} \, \mathrm{d}x$$

$$- \sum_{i,j=1}^{N} \int_{\Omega_i} (f \, p)_{j-1/2} \, \psi_{j-1/2}^{+} \, \mathrm{d}x + \sum_{i,j=1}^{N} \int_{\Omega_{ij}} f(u) \, (p \, \psi)_y \, \mathrm{d}x \, \mathrm{d}y - \sum_{i,j=1}^{N} \int_{\Omega_i} (f)_{j+1/2} \, p_{j+1/2}^{-} \, \psi_{j+1/2}^{-} \, \mathrm{d}x$$

$$+ \sum_{i,j=1}^{N} \int_{\Omega_i} (f)_{j-1/2} \, p_{j-1/2}^{+} \, \psi_{j-1/2}^{+} \, \mathrm{d}x - \sum_{i,j=1}^{N} \int_{\Omega_{ij}} p \, v \, \psi \, \mathrm{d}x \, \mathrm{d}y = 0, \quad (2.7)$$

and

$$\sum_{i,j=1}^{N} \int_{\Omega_{ij}} u_t \, \zeta \, \mathrm{d}x \, \mathrm{d}y = \sum_{i,j=1}^{N} \int_{\Omega_{ij}} p \, \zeta \, \mathrm{d}x \, \mathrm{d}y. \quad (2.8)$$

Remark 2.1. *Admittedly, the notation used in (2.5)–(2.8) is more cumbersome than the vector notation often seen in the DG literature. The purpose of this is to be able to treat the fluxes in the different equations differently in order to ensure energy conservation.*

In order to complete the description of the above schemes, we need to specify numerical flux functions.

2.4. **Energy Preserving Scheme.** For a conservative scheme, we use the central numerical flux

$$(f)_{k\pm 1/2} = \overline{f}_{k\pm 1/2} \quad \text{and} \quad (fg)_{k\pm 1/2} = \overline{f}_{k\pm 1/2} \overline{g}_{k\pm 1/2},$$

for any grid functions $f, g \in X_h^s(\Omega)$. An energy preserving RK-DG scheme based on the weak formulation (2.5)–(2.8) becomes: Find $p, v, w, u \in X_h^s(\Omega)$ such that

$$\sum_{i,j=1}^{N} \int_{\Omega_{ij}} p_t \, \phi \, \mathrm{d}x \, \mathrm{d}y + \alpha \sum_{i,j=1}^{N} \int_{\Omega_{ij}} f(u) \, v \, \phi_x \, \mathrm{d}x \, \mathrm{d}y - \alpha \sum_{i,j=1}^{N} \int_{\Omega_j} \overline{f}_{i+1/2} \, \overline{v}_{i+1/2} \, \phi_{i+1/2}^{-} \, \mathrm{d}y$$

$$+ \alpha \sum_{i,j=1}^{N} \int_{\Omega_j} \overline{f}_{i-1/2} \, \overline{v}_{i-1/2} \, \phi_{i-1/2}^{+} \, \mathrm{d}y + \alpha \sum_{i,j=1}^{N} \int_{\Omega_{ij}} g(u) \, v \, \phi_y \, \mathrm{d}x \, \mathrm{d}y - \alpha \sum_{i,j=1}^{N} \int_{\Omega_i} \overline{g}_{j+1/2} \, \overline{v}_{j+1/2} \, \phi_{j+1/2}^{-} \, \mathrm{d}x$$

$$+ \alpha \sum_{i,j=1}^{N} \int_{\Omega_i} \overline{g}_{j-1/2} \, \overline{v}_{j-1/2} \, \phi_{j-1/2}^{+} \, \mathrm{d}x + \beta \sum_{i,j=1}^{N} \int_{\Omega_{ij}} g(u) \, w \, \phi_x \, \mathrm{d}x \, \mathrm{d}y - \beta \sum_{i,j=1}^{N} \int_{\Omega_j} \overline{g}_{i+1/2} \, \overline{w}_{i+1/2} \, \phi_{i+1/2}^{-} \, \mathrm{d}y$$

$$+ \beta \sum_{i,j=1}^{N} \int_{\Omega_j} \overline{g}_{i-1/2} \, \overline{w}_{i-1/2} \, \phi_{i-1/2}^{+} \, \mathrm{d}y - \beta \sum_{i,j=1}^{N} \int_{\Omega_j} f(u) \, w \, \phi_y \, \mathrm{d}x \, \mathrm{d}y + \beta \sum_{i,j=1}^{N} \int_{\Omega_i} \overline{f}_{j+1/2} \, \overline{w}_{j+1/2} \, \phi_{j+1/2}^{-} \, \mathrm{d}x$$

$$- \beta \sum_{i,j=1}^{N} \int_{\Omega_i} \overline{f}_{j-1/2} \, \overline{w}_{j-1/2} \, \phi_{j-1/2}^{+} \, \mathrm{d}x - \alpha \sum_{i,j=1}^{N} \int_{\Omega_{ij}} v \, w \, \phi \, \mathrm{d}x \, \mathrm{d}y + \beta \sum_{i,j=1}^{N} \int_{\Omega_{ij}} v \, w \, \phi \, \mathrm{d}x \, \mathrm{d}y = 0,$$

$$(2.9)$$

for all $\phi \in X_{\Delta x}^s(\Omega)$,

$$\sum_{i,j=1}^{N} \int_{\Omega_{ij}} v_t \, \nu \, \mathrm{d}x \, \mathrm{d}y + \sum_{i,j=1}^{N} \int_{\Omega_{ij}} f(u) \, p \, \nu_x \, \mathrm{d}x \, \mathrm{d}y - \sum_{i,j=1}^{N} \int_{\Omega_j} \overline{f}_{i+1/2} \, \overline{p}_{i+1/2} \, \nu_{i+1/2}^{-} \, \mathrm{d}y$$

$$+ \sum_{i,j=1}^{N} \int_{\Omega_j} \overline{f}_{i-1/2} \, \overline{p}_{i-1/2} \, \nu_{i-1/2}^{+} \, \mathrm{d}y - \sum_{i,j=1}^{N} \int_{\Omega_{ij}} f(u) \, (p\,\nu)_x \, \mathrm{d}x \, \mathrm{d}y + \sum_{i,j=1}^{N} \int_{\Omega_j} \overline{f}_{i+1/2} \, p_{i+1/2}^{-} \, \nu_{i+1/2}^{-} \, \mathrm{d}y$$

$$- \sum_{i,j=1}^{N} \int_{\Omega_j} \overline{f}_{i-1/2} \, p_{i-1/2}^{+} \, \nu_{i-1/2}^{+} \, \mathrm{d}y + \sum_{i,j=1}^{N} \int_{\Omega_{ij}} g(u) \, p \, \nu_y \, \mathrm{d}x \, \mathrm{d}y - \sum_{i,j=1}^{N} \int_{\Omega_i} \overline{g}_{j+1/2} \, \overline{p}_{j+1/2} \, \nu_{j+1/2}^{-} \, \mathrm{d}x$$

$$+ \sum_{i,j=1}^{N} \int_{\Omega_i} \overline{g}_{j-1/2} \, \overline{p}_{j-1/2} \, \nu_{j-1/2}^{+} \, \mathrm{d}x - \sum_{i,j=1}^{N} \int_{\Omega_{ij}} g(u) \, (p\,\nu)_y \, \mathrm{d}x \, \mathrm{d}y + \sum_{i,j=1}^{N} \int_{\Omega_i} \overline{g}_{j+1/2} \, p_{j+1/2}^{-} \, \nu_{j+1/2}^{-} \, \mathrm{d}x$$

$$- \sum_{i,j=1}^{N} \int_{\Omega_i} \overline{g}_{j-1/2} \, p_{j-1/2}^{+} \, \nu_{j-1/2}^{+} \, \mathrm{d}x + \sum_{i,j=1}^{N} \int_{\Omega_{ij}} p \, w \, \nu \, \mathrm{d}x \, \mathrm{d}y = 0, \quad (2.10)$$

for all $\nu \in X_h^s(\Omega)$,

$$\sum_{i,j=1}^{N} \int_{\Omega_{ij}} w_t \, \psi \, \mathrm{d}x \, \mathrm{d}y + \sum_{i,j=1}^{N} \int_{\Omega_{ij}} g(u) \, p \, \psi_x \, \mathrm{d}x \, \mathrm{d}y - \sum_{i,j=1}^{N} \int_{\Omega_j} \overline{g}_{i+1/2} \, \overline{p}_{i+1/2} \, \psi_{i+1/2}^{-} \, \mathrm{d}y$$

$$+ \sum_{i,j=1}^{N} \int_{\Omega_j} \overline{g}_{i-1/2} \, \overline{p}_{i-1/2} \, \psi_{i-1/2}^{+} \, \mathrm{d}y - \sum_{i,j=1}^{N} \int_{\Omega_{ij}} g(u) \, (p\,\psi)_x \, \mathrm{d}x \, \mathrm{d}y + \sum_{i,j=1}^{N} \int_{\Omega_j} \overline{g}_{i+1/2} \, p_{i+1/2}^{-} \, \psi_{i+1/2}^{-} \, \mathrm{d}y$$

$$- \sum_{i,j=1}^{N} \int_{\Omega_j} \overline{g}_{i-1/2} \, p_{i-1/2}^{+} \, \psi_{i-1/2}^{+} \, \mathrm{d}y - \sum_{i,j=1}^{N} \int_{\Omega_{ij}} f(u) \, p \, \psi_y \, \mathrm{d}x \, \mathrm{d}y + \sum_{i,j=1}^{N} \int_{\Omega_i} \overline{f}_{j+1/2} \, \overline{p}_{j+1/2} \, \psi_{j+1/2}^{-} \, \mathrm{d}x$$

$$- \sum_{i,j=1}^{N} \int_{\Omega_i} \overline{f}_{j-1/2} \, \overline{p}_{j-1/2} \, \psi_{j-1/2}^{+} \, \mathrm{d}x + \sum_{i,j=1}^{N} \int_{\Omega_{ij}} f(u) \, (p\,\psi)_y \, \mathrm{d}x \, \mathrm{d}y - \sum_{i,j=1}^{N} \int_{\Omega_i} \overline{f}_{j+1/2} \, p_{j+1/2}^{-} \, \psi_{j+1/2}^{-} \, \mathrm{d}x$$

$$+ \sum_{i,j=1}^{N} \int_{\Omega_i} \overline{f}_{j-1/2} \, p_{j-1/2}^{+} \, \psi_{j-1/2}^{+} \, \mathrm{d}x - \sum_{i,j=1}^{N} \int_{\Omega_{ij}} p \, v \, \psi \, \mathrm{d}x \, \mathrm{d}y = 0, \quad (2.11)$$

for all $\psi \in X_h^s(\Omega)$ and

$$\sum_{i,j=1}^{N} \int_{\Omega_{ij}} u_t \, \zeta \, \mathrm{d}x \, \mathrm{d}y = \sum_{i,j=1}^{N} \int_{\Omega_{ij}} p \, \zeta \, \mathrm{d}x \, \mathrm{d}y. \quad (2.12)$$

for all $\zeta \in X_h^s(\Omega)$.

The above scheme preserves a discrete version of the energy, as shown in the following theorem:

Theorem 2.1. *Let p, v and w be approximate solutions generated by the scheme* (2.9)–(2.12) *with periodic boundary conditions. Then*

$$\frac{d}{dt} \sum_{i,j=1}^{N} \int_{\Omega_{ij}} \left(p^2(t) + \alpha \, v^2(t) + \beta \, w^2(t) \right) \, \mathrm{d}x \, \mathrm{d}y = 0.$$

Proof. Let p, v and w be numerical solutions generated by the scheme (2.9)–(2.12). Since those equations hold for any $\phi, \nu, \psi \in X_h^s(\Omega)$, they hold in particular for $\phi = p, \nu = v$ and $\psi = w$. We can then calculate

$$\frac{d}{dt} \sum_{i,j=1}^{N} \int_{\Omega_{ij}} \left(p^2(t) + \alpha \, v^2(t) + \beta \, w^2(t) \right) \, \mathrm{d}x \, \mathrm{d}y = 2 \sum_{i,j=1}^{N} \int_{\Omega_{ij}} \left(p p_t + \alpha \, v v_t + \beta \, w w_t \right) \, \mathrm{d}x \, \mathrm{d}y$$

$$= 2\alpha \sum_{i,j=1}^{N} \int_{\Omega_j} \overline{f}_{i+1/2} \left(\overline{v}_{i+1/2} [\![p]\!]_{i+1/2} + \overline{p}_{i+1/2} [\![v]\!]_{i+1/2} - [\![pv]\!]_{i+1/2} \right) \, \mathrm{d}y$$

$$+ 2\alpha \sum_{i,j=1}^{N} \int_{\Omega_i} \overline{g}_{j+1/2} \left(\overline{v}_{j+1/2} [\![p]\!]_{j+1/2} + \overline{p}_{j+1/2} [\![v]\!]_{j+1/2} - [\![pv]\!]_{j+1/2} \right) \mathrm{d}x$$

$$+ 2\beta \sum_{i,j=1}^{N} \int_{\Omega_j} \overline{g}_{i+1/2} \left(\overline{v}_{i+1/2} [\![p]\!]_{i+1/2} + \overline{p}_{i+1/2} [\![w]\!]_{i+1/2} - [\![pw]\!]_{i+1/2} \right) \mathrm{d}y$$

$$+ 2\alpha \sum_{i,j=1}^{N} \int_{\Omega_i} \overline{f}_{j+1/2} \left(-\overline{w}_{j+1/2} [\![p]\!]_{j+1/2} - \overline{p}_{j+1/2} [\![w]\!]_{j+1/2} + [\![pw]\!]_{j+1/2} \right) \mathrm{d}x = 0,$$

where we have used the periodic boundary conditions and the identities (2.4). $\qquad\square$

Remark 2.2. *Theorem 2.1 and similar results to follow explicitly assume periodic boundary conditions. It is however straightforward to show that these results also hold for certain other situations such as with compactly supported or decaying data.*

2.5. **Energy Dissipating Scheme.** Note that the above designed energy conservative scheme (2.9)–(2.12) is expected to approximate a conservative solution of the underlying system (1.6). To attempt to approximate a dissipative solution of (1.6), one has to add *numerical viscosity.* In this work we propose adding viscosity in the numerical fluxes (scaled by the maximum wave speed) as well as a *shock capturing operator* dissipating energy near shocks or discontinuities. Specifically, we propose the following modification of the energy conservative scheme (2.9)–(2.12):

Denoting
$$s_{i\pm 1/2} = \max\{c_{i\pm 1/2}^-, c_{i\pm 1/2}^+\} \text{ and } s_{j\pm 1/2} = \max\{b_{j\pm 1/2}^-, b_{j\pm 1/2}^+\}$$

for the maximal local wave velocity, a dissipative version of the DG scheme is then given by the following: Find $p, v, w, u \in X_h^s(\Omega)$ such that

$$\sum_{i,j=1}^{N} \int_{\Omega_{ij}} p_t\, \phi\, \mathrm{d}x\, \mathrm{d}y + \alpha \sum_{i,j=1}^{N} \int_{\Omega_{ij}} f(u)\, v\, \phi_x\, \mathrm{d}x\, \mathrm{d}y$$

$$- \alpha \sum_{i,j=1}^{N} \int_{\Omega_j} \underbrace{\left(\overline{f}_{i+1/2}\, \overline{v}_{i+1/2} + \frac{1}{2} s_{i+1/2} [\![p]\!]_{i+1/2} \right)}_{\text{diffusive flux in x-direction}} \phi_{i+1/2}^-\, \mathrm{d}y$$

$$+ \alpha \sum_{i,j=1}^{N} \int_{\Omega_j} \underbrace{\left(\overline{f}_{i-1/2}\, \overline{v}_{i-1/2} + \frac{1}{2} s_{i-1/2} [\![p]\!]_{i-1/2} \right)}_{\text{diffusive flux in x-direction}} \phi_{i-1/2}^+\, \mathrm{d}y$$

$$+ \alpha \sum_{i,j=1}^{N} \int_{\Omega_{ij}} g(u)\, v\, \phi_y\, \mathrm{d}x\, \mathrm{d}y - \alpha \sum_{i,j=1}^{N} \int_{\Omega_i} \underbrace{\left(\overline{g}_{j+1/2}\, \overline{v}_{j+1/2} + \frac{1}{2} s_{j+1/2} [\![p]\!]_{j+1/2} \right)}_{\text{diffusive flux in y-direction}} \phi_{j+1/2}^-\, \mathrm{d}x$$

$$+ \alpha \sum_{i,j=1}^{N} \int_{\Omega_i} \underbrace{\left(\overline{g}_{j-1/2}\, \overline{v}_{j-1/2} + \frac{1}{2} s_{j-1/2} [\![p]\!]_{j-1/2} \right)}_{\text{diffusive flux in y-direction}} \phi_{j-1/2}^+\, \mathrm{d}x + \beta \sum_{i,j=1}^{N} \int_{\Omega_{ij}} g(u)\, w\, \phi_x\, \mathrm{d}x\, \mathrm{d}y$$

$$- \beta \sum_{i,j=1}^{N} \int_{\Omega_j} \overline{g}_{i+1/2}\, \overline{w}_{i+1/2}\, \phi_{i+1/2}^-\, \mathrm{d}y + \beta \sum_{i,j=1}^{N} \int_{\Omega_j} \overline{g}_{i-1/2}\, \overline{w}_{i-1/2}\, \phi_{i-1/2}^+\, \mathrm{d}y - \beta \sum_{i,j=1}^{N} \int_{\Omega_j} f(u)\, w\, \phi_y\, \mathrm{d}x\, \mathrm{d}y$$

$$+ \beta \sum_{i,j=1}^{N} \int_{\Omega_i} \overline{f}_{j+1/2}\, \overline{w}_{j+1/2}\, \phi_{j+1/2}^-\, \mathrm{d}x - \beta \sum_{i,j=1}^{N} \int_{\Omega_i} \overline{f}_{j-1/2}\, \overline{w}_{j-1/2}\, \phi_{j-1/2}^+\, \mathrm{d}x - \alpha \sum_{i,j=1}^{N} \int_{\Omega_{ij}} v\, w\, \phi\, \mathrm{d}x\, \mathrm{d}y$$

$$+ \beta \sum_{i,j=1}^{N} \int_{\Omega_{ij}} v\, w\, \phi\, \mathrm{d}x\, \mathrm{d}y = - \sum_{i,j=1}^{N} \varepsilon_{ij} \underbrace{\int_{\Omega_{ij}} (p_x\, \phi_x + p_y\, \phi_y)\, \mathrm{d}x\, \mathrm{d}y}_{\text{shock capturing operator}}, \quad (2.13)$$

for all $\phi \in X_h^s(\Omega)$,

$$
\sum_{i,j=1}^{N} \int_{\Omega_{ij}} v_t \, \nu \, \mathrm{d}x \, \mathrm{d}y + \sum_{i,j=1}^{N} \int_{\Omega_{ij}} f(u) \, p \, \nu_x \, \mathrm{d}x \, \mathrm{d}y - \sum_{i,j=1}^{N} \int_{\Omega_j} \underbrace{\left(\overline{f}_{i+1/2} \, \overline{p}_{i+1/2} + \frac{1}{2} s_{i+1/2} [\![v]\!]_{i+1/2} \right)}_{\text{diffusive flux in x-direction}} \nu_{i+1/2}^{-} \, \mathrm{d}y
$$

$$
+ \sum_{i,j=1}^{N} \int_{\Omega_j} \underbrace{\left(\overline{f}_{i-1/2} \, \overline{p}_{i-1/2} + \frac{1}{2} s_{i-1/2} [\![v]\!]_{i-1/2} \right)}_{\text{diffusive flux in x-direction}} \nu_{i-1/2}^{+} \, \mathrm{d}y
$$

$$
- \sum_{i,j=1}^{N} \int_{\Omega_{ij}} f(u) \, (p \, \nu)_x \, \mathrm{d}x \, \mathrm{d}y + \sum_{i,j=1}^{N} \int_{\Omega_j} \overline{f}_{i+1/2} \, p_{i+1/2}^{-} \, \nu_{i+1/2}^{-} \, \mathrm{d}y
$$

$$
- \sum_{i,j=1}^{N} \int_{\Omega_j} \overline{f}_{i-1/2} \, p_{i-1/2}^{+} \, \nu_{i-1/2}^{+} \, \mathrm{d}y + \sum_{i,j=1}^{N} \int_{\Omega_{ij}} g(u) \, p \, \nu_y \, \mathrm{d}x \, \mathrm{d}y
$$

$$
- \sum_{i,j=1}^{N} \int_{\Omega_i} \underbrace{\left(\overline{g}_{j+1/2} \, \overline{p}_{j+1/2} + \frac{1}{2} s_{j+1/2} [\![v]\!]_{j+1/2} \right)}_{\text{diffusive flux in y-direction}} \nu_{j+1/2}^{-} \, \mathrm{d}x
$$

$$
+ \sum_{i,j=1}^{N} \int_{\Omega_i} \underbrace{\left(\overline{g}_{j-1/2} \, \overline{p}_{j-1/2} + \frac{1}{2} s_{j-1/2} [\![v]\!]_{j-1/2} \right)}_{\text{diffusive flux in y-direction}} \nu_{j-1/2}^{+} \, \mathrm{d}x
$$

$$
- \sum_{i,j=1}^{N} \int_{\Omega_{ij}} g(u) \, (p \, \nu)_y \, \mathrm{d}x \, \mathrm{d}y + \sum_{i,j=1}^{N} \int_{\Omega_i} \overline{g}_{j+1/2} \, p_{j+1/2}^{-} \, \nu_{j+1/2}^{-} \, \mathrm{d}x
$$

$$
- \sum_{i,j=1}^{N} \int_{\Omega_i} \overline{g}_{j-1/2} \, p_{j-1/2}^{+} \, \nu_{j-1/2}^{+} \, \mathrm{d}x + \sum_{i,j=1}^{N} \int_{\Omega_{ij}} p \, w \, \nu \, \mathrm{d}x \, \mathrm{d}y = - \sum_{i,j=1}^{N} \varepsilon_{ij} \underbrace{\int_{\Omega_{ij}} (v_x \, \nu_x + v_y \, \nu_y) \, \mathrm{d}x \, \mathrm{d}y}_{\text{shock capturing operator}},
$$

$$\tag{2.14}$$

for all $\nu \in X_h^s(\Omega)$,

$$
\sum_{i,j=1}^{N} \int_{\Omega_{ij}} w_t \, \psi \, \mathrm{d}x \, \mathrm{d}y + \sum_{i,j=1}^{N} \int_{\Omega_{ij}} g(u) \, p \, \psi_x \, \mathrm{d}x \, \mathrm{d}y
$$

$$
- \sum_{i,j=1}^{N} \int_{\Omega_j} \underbrace{\left(\overline{g}_{i+1/2} \, \overline{p}_{i+1/2} + \frac{1}{2} s_{i+1/2} [\![w]\!]_{i+1/2} \right)}_{\text{diffusive flux in x-direction}} \psi_{i+1/2}^{-} \, \mathrm{d}y
$$

$$
+ \sum_{i,j=1}^{N} \int_{\Omega_j} \underbrace{\left(\overline{g}_{i-1/2} \, \overline{p}_{i-1/2} + \frac{1}{2} s_{i-1/2} [\![w]\!]_{i-1/2} \right)}_{\text{diffusive flux in x-direction}} \psi_{i-1/2}^{+} \, \mathrm{d}y
$$

$$
- \sum_{i,j=1}^{N} \int_{\Omega_{ij}} g(u) \, (p \, \psi)_x \, \mathrm{d}x \, \mathrm{d}y + \sum_{i,j=1}^{N} \int_{\Omega_j} \overline{g}_{i+1/2} \, p_{i+1/2}^{-} \, \psi_{i+1/2}^{-} \, \mathrm{d}y
$$

$$
- \sum_{i,j=1}^{N} \int_{\Omega_j} \overline{g}_{i-1/2} \, p_{i-1/2}^{+} \, \psi_{i-1/2}^{+} \, \mathrm{d}y - \sum_{i,j=1}^{N} \int_{\Omega_{ij}} f(u) \, p \, \psi_y \, \mathrm{d}x \, \mathrm{d}y
$$

$$+ \sum_{i,j=1}^{N} \int_{\Omega_i} \underbrace{\left(\overline{f}_{j+1/2}\,\overline{p}_{j+1/2} - \frac{1}{2}s_{j+1/2}[\![w]\!]_{j+1/2} \right)}_{\text{diffusive flux in y-direction}} \psi_{j+1/2}^{-}\,\mathrm{d}x$$

$$- \sum_{i,j=1}^{N} \int_{\Omega_i} \underbrace{\left(\overline{f}_{j-1/2}\,\overline{p}_{j-1/2} - \frac{1}{2}s_{j-1/2}[\![w]\!]_{j-1/2} \right)}_{\text{diffusive flux in y-direction}} \psi_{j-1/2}^{+}\,\mathrm{d}x$$

$$+ \sum_{i,j=1}^{N} \int_{\Omega_{ij}} f(u)\,(p\,\psi)_y\,\mathrm{d}x\,\mathrm{d}y - \sum_{i,j=1}^{N} \int_{\Omega_i} \overline{f}_{j+1/2}\,p_{j+1/2}^{-}\,\psi_{j+1/2}^{-}\,\mathrm{d}x$$

$$+ \sum_{i,j=1}^{N} \int_{\Omega_i} \overline{f}_{j-1/2}\,p_{j-1/2}^{+}\,\psi_{j-1/2}^{+}\,\mathrm{d}x - \sum_{i,j=1}^{N} \int_{\Omega_{ij}} p\,v\,\psi\,\mathrm{d}x\,\mathrm{d}y = - \underbrace{\sum_{i,j=1}^{N} \varepsilon_{ij} \int_{\Omega_{ij}} (w_x\,\psi_x + w_y\,\psi_y)\,\mathrm{d}x\,\mathrm{d}y,}_{\text{shock capturing operator}}$$

$$(2.15)$$

for all $\psi \in X_h^s(\Omega)$,

$$\sum_{i,j=1}^{N} \int_{\Omega_{ij}} u_t\,\zeta\,\mathrm{d}x\,\mathrm{d}y = \sum_{i,j=1}^{N} \int_{\Omega_{ij}} p\,\zeta\,\mathrm{d}x\,\mathrm{d}y. \qquad (2.16)$$

for all $\zeta \in X_h^s(\Omega)$.

The scaling parameter ε in the *shock capturing operator* is given by

$$\varepsilon_{ij} = \frac{h_{ij}\,C\,\overline{\mathrm{Res}}}{\left(\int_{\Omega_{ij}} (p_x^2 + v_x^2 + w_x^2)\mathrm{d}x\,\mathrm{d}y + \int_{\Omega_{ij}} (p_y^2 + v_y^2 + w_y^2)\mathrm{d}x\,\mathrm{d}y \right)^{1/2} + h_{ij}^{\theta}} \qquad (2.17)$$

where $C > 0$ is a constant, $\theta \geq 1/2$, $h_{ij} = \max\{\Delta x_{ij}, \Delta y_{ij}\}$ and

$$\overline{\mathrm{Res}} = \left(\int_{\Omega_{ij}} (\mathrm{Res})^2 \mathrm{d}x\,\mathrm{d}y \right)^{1/2} \qquad (2.18)$$

with

$$\mathrm{Res} = \left(p^2 + \alpha\,v^2 + \beta\,w^2 \right)_t + \left(\alpha\,p\,f(u)\,v + \beta\,p\,g(u)\,w \right)_x + \left(\alpha\,p\,g(u)\,v - \beta\,p\,f(u)\,w \right)_y. \qquad (2.19)$$

The rationale for the scaling parameter is as follows: For smooth solutions of (2.1) the conservation law (2.3) is fulfilled. The numerical solution is then expected to fulfill the same conservation law up to the spatial and temporal accuracy of the scheme. The shock capturing operator will therefore vanish in smooth regions, while introducing added dissipation near shocks and discontinuities.

The above scheme dissipates a discrete version of the energy, as shown in the following theorem:

Theorem 2.2. *Let p, v and w be approximate solutions generated by the scheme (2.9)–(2.12) with periodic boundary conditions. Then*

$$\frac{d}{dt} \sum_{i,j=1}^{N} \int_{\Omega_{ij}} \left(p^2(t) + \alpha\,v^2(t) + \beta\,w^2(t) \right)\,\mathrm{d}x\,\mathrm{d}y \leq 0.$$

Proof. By using the result from Theorem 2.1, we can write

$$\frac{d}{dt} \sum_{i,j=1}^{N} \int_{\Omega_{ij}} \left(p^2(t) + \alpha\, v^2(t) + \beta\, w^2(t) \right) \, dx\, dy$$

$$= -2 \sum_{i,j=1}^{N} \varepsilon_{ij} \int_{\Omega_{ij}} \left(p_x^2 + p_y^2 + v_x^2 + v_y^2 + w_x^2 + w_y^2 \right) dx\, dy$$

$$+ \alpha \sum_{i,j=1}^{N} \int_{\Omega_j} \left(s_{i+1/2} [\![p]\!]_{i+1/2} p_{i+1/2}^- - s_{i-1/2} [\![p]\!]_{i-1/2} p_{i-1/2}^+ \right) dy$$

$$+ \alpha \sum_{i,j=1}^{N} \int_{\Omega_i} \left(s_{j+1/2} [\![p]\!]_{j+1/2} p_{j+1/2}^- - s_{j-1/2} [\![p]\!]_{j-1/2} p_{j-1/2}^+ \right) dx$$

$$+ \alpha \sum_{i,j=1}^{N} \int_{\Omega_j} \left(s_{i+1/2} [\![v]\!]_{i+1/2} v_{i+1/2}^- - s_{i-1/2} [\![v]\!]_{i-1/2} v_{i-1/2}^+ \right) dy \tag{2.20}$$

$$+ \alpha \sum_{i,j=1}^{N} \int_{\Omega_i} \left(s_{j+1/2} [\![v]\!]_{j+1/2} v_{j+1/2}^- - s_{j-1/2} [\![v]\!]_{j-1/2} v_{j-1/2}^+ \right) dx$$

$$+ \beta \sum_{i,j=1}^{N} \int_{\Omega_j} \left(s_{i+1/2} [\![w]\!]_{i+1/2} w_{i+1/2}^- - s_{i-1/2} [\![w]\!]_{i-1/2} w_{i-1/2}^+ \right) dy$$

$$+ \beta \sum_{i,j=1}^{N} \int_{\Omega_i} \left(s_{j+1/2} [\![w]\!]_{j+1/2} w_{j+1/2}^- - s_{j-1/2} [\![w]\!]_{j-1/2} w_{j-1/2}^+ \right) dx$$

Now, since the periodic boundary condition lends the relation

$$\sum_{i,j=1}^{N} \left(s_{i+1/2} [\![a]\!]_{i+1/2} a_{i+1/2}^- - s_{i-1/2} [\![a]\!]_{i-1/2} a_{i-1/2}^+ \right) = - \sum_{i,j=1}^{N} s_{i+1/2} [\![a]\!]_{i+1/2}^2, \tag{2.21}$$

we can write

$$\frac{d}{dt} \sum_{i,j=1}^{N} \int_{\Omega_{ij}} \left(p^2(t) + \alpha\, v^2(t) + \beta\, w^2(t) \right) \, dx\, dy$$

$$= -2 \sum_{i,j=1}^{N} \varepsilon_{ij} \int_{\Omega_{ij}} \left(p_x^2 + p_y^2 + v_x^2 + v_y^2 + w_x^2 + w_y^2 \right) dx\, dy$$

$$- \alpha \sum_{i,j=1}^{N} \int_{\Omega_j} s_{i+1/2} [\![p]\!]_{i+1/2}^2 dy - \alpha \sum_{i,j=1}^{N} \int_{\Omega_i} s_{j+1/2} [\![p]\!]_{j+1/2}^2 dx \tag{2.22}$$

$$- \alpha \sum_{i,j=1}^{N} \int_{\Omega_j} s_{i+1/2} [\![v]\!]_{i+1/2}^2 dy - \alpha \sum_{i,j=1}^{N} \int_{\Omega_i} s_{j+1/2} [\![v]\!]_{j+1/2}^2 dx$$

$$- \beta \sum_{i,j=1}^{N} \int_{\Omega_j} s_{i+1/2} [\![w]\!]_{i+1/2}^2 dy - \beta \sum_{i,j=1}^{N} \int_{\Omega_i} s_{j+1/2} [\![w]\!]_{j+1/2}^2 dx.$$

The result then follows from the positivity of ε_{ij}, s and the physical parameters α and β. $\qquad \square$

3. Energy Preserving Scheme Based On a Variational Formulation

It is worth noting that all the previous schemes were designed by rewriting the variational wave equation (1.6) as first-order systems and approximating these systems. However, one can also design a scheme for the original variational wave equation (1.6). To achieve this, we design

an energy conservative scheme by approximating the nonlinear wave equation (1.6) directly. We proceed by rewriting the nonlinear wave equation (1.6) in the general form:

$$u_{tt} = -\frac{\delta H}{\delta u}, \tag{3.1}$$

with

$$H = H(u, u_x, u_y) := \frac{1}{2}\, c^2(u)\, u_x^2 + \frac{1}{2}\, b^2(u)\, u_y^2 + a(u)\, u_x\, u_y.$$

Here, H is the "Hamiltonian", and $\frac{\delta H}{\delta u}$ denotes the variational derivative of function $H(u, u_x, u_y)$ with respect to u.

A simple calculation, in light of (3.1), reveals that

$$\frac{d}{dt} \int_{\mathbb{R}} \left(\frac{1}{2} u_t^2 + H(u, u_x, u_y) \right)\, dx = 0. \tag{3.2}$$

To be more precise, this is a direct consequence of the simple identity:

$$\frac{\delta H}{\delta u} = \frac{\partial H}{\partial u} - \frac{d}{dx}\left(\frac{\partial H}{\partial u_x}\right) - \frac{d}{dy}\left(\frac{\partial H}{\partial u_y}\right). \tag{3.3}$$

We also note that for equation (1.6),

$$\frac{\delta H}{\delta u} = c(u)c'(u)u_x^2 - \left(c^2(u)u_x\right)_x + b(u)b'(u)u_y^2 - \left(b^2(u)u_y\right)_y + a'(u)u_x u_y - (a(u)u_y)_x - (a(u)u_x)_y$$

$$= -c^2(u)u_{xx} - c(u)c'(u)u_x^2 - b^2(u)u_{yy} - b(u)b'(u)u_y^2 - a'(u)u_x u_y - 2a(u)u_{xy}$$

$$= -c(u)\left(c(u)u_x\right)_x - b(u)\left(b(u)u_y\right)_y - a'(u)u_x u_y - 2a(u)u_{xy}.$$

Based on above observations, we propose the following scheme for (1.6)

$$(u_{ij})_{tt} + c(u_{ij})c'(u_{ij})(D^x u_{ij})^2 - D^x\left(c^2(u_{ij})D^x u_{ij}\right) + b(u_{ij})b'(u_{ij})(D^y u_{ij})^2 - D^y\left(b^2(u_{ij})D^y u_{ij}\right)$$

$$+ a'(u_{ij})D^x(u_{ij})D^y(u_{ij}) - D^x\left(a(u_{ij})D^y u_{ij}\right) - D^y\left(a(u_{ij})D^x u_{ij}\right) = 0, \tag{3.4}$$

where the central differences D^x and D^y are defined by

$$D^x z_{ij} = \frac{z_{i+1,j} - z_{i-1,j}}{2\Delta x}, \text{ and } D^y z_{ij} = \frac{z_{i,j+1} - z_{i,j-1}}{2\Delta y}.$$

This scheme is energy preserving as shown in the following theorem:

Theorem 3.1. *Let $u_{ij}(t)$ be an approximate solution generated by the scheme (3.4) using periodic boundary conditions. Then we have*

$$\frac{d}{dt}\left(\frac{\Delta x\Delta y}{2}\sum_{i,j}(u_{ij})_t^2 + c^2(u_{ij})\left(D^x u_{ij}\right)^2 + b^2(u_{ij})\left(D^y u_{ij}\right)^2 + 2a(u_{ij})D^x(u_{ij})D^y(u_{ij})\right) = 0.$$

Proof. We start by calculating

$$\frac{d}{dt}\left(\frac{\Delta x\Delta y}{2}\sum_{i,j}(u_{ij})_t^2 + c^2(u_{ij})\left(D^x u_{ij}\right)^2 + b^2(u_{ij})\left(D^y u_{ij}\right)^2 + 2a(u_{ij})D^x(u_{ij})D^y(u_{ij})\right)$$

$$= \Delta x\Delta y \sum_{i,j}\left((u_{ij})_t(u_{ij})_{tt} + c(u_{ij})c'(u_{ij})\left(D^x u_{ij}\right)^2(u_{ij})_t + c^2(u_{ij})D^x u_{ij}D^x(u_{ij})_t\right)$$

$$+ \Delta x\Delta y \sum_{i,j}\left(b(u_{ij})b'(u_{ij})\left(D^y u_{ij}\right)^2(u_{ij})_t + b^2(u_{ij})D^y u_{ij}D^y(u_{ij})_t\right)$$

$$+ \Delta x\Delta y \sum_{i,j}\left(a'(u_{ij})D^x(u_{ij})D^y(u_{ij})(u_{ij})_t + a(u_{ij})D^x(u_{ij})_t D^y u_{ij} + a(u_{ij})D^x u_{ij}D^y(u_{ij})_t\right)$$

$$= \Delta x\Delta y \sum_{i,j}\left((u_{ij})_t(u_{ij})_{tt} + c(u_{ij})c'(u_{ij})\left(D^x u_{ij}\right)^2(u_{ij})_t - D^x\left(c^2(u_{ij})D^x u_{ij}\right)(u_{ij})_t\right)$$

$$+ \Delta x \Delta y \sum_{i,j} \left(b(u_{ij}) b'(u_{ij}) \left(D^y u_{ij} \right)^2 (u_{ij})_t - D^y \left(b^2(u_{ij}) D^y u_{ij} \right) (u_{ij})_t \right)$$

$$+ \Delta x \Delta y \sum_{i,j} \left(a'(u_{ij}) D^x(u_{ij}) D^y(u_{ij})(u_{ij})_t - D^x \left(a(u_{ij}) D^y u_{ij} \right) (u_{ij})_t - D^y \left(a(u_{ij}) D^x u_{ij} \right) (u_{ij})_t \right)$$

$$= 0. \text{ (follows from (3.4))}$$

$\square$

4. NUMERICAL EXPERIMENTS

For the numerical experiments, the computational domain is subdivided into $N \times N$ rectangular cells. All cells are of size $\Delta x \times \Delta y$. A uniform time step

$$\Delta t = 0.1 \frac{\min\{\Delta x, \Delta y\}}{\max\{\alpha, \beta\}} \tag{4.1}$$

is used throughout the computation. Moreover, in all experiments the parameters for the shock capturing operator are $C = 0.1$ and $\theta = 1$. To keep focus on the spatial discretization, we will use a fifth-order Runge–Kutta scheme [22] ensuring a satisfactory temporal accuracy. Periodic boundary conditions are used in all experiments.

4.1. **Gaussian disturbance to homogeneous director state.** In this section we consider the initial value problem (1.6) with the initial data

$$u_0(x, y) = \exp\left(-16\left(x^2 + y^2\right)\right) \tag{4.2a}$$

$$u_1(x, y) = 0 \tag{4.2b}$$

on $(x, y) \in \mathbb{R}^2$. The physical parameters are $\alpha = 1.5$ and $\beta = 0.5$. A numerical solution was computed using $N = 32$ with the dissipative piecewise quadratic ($s = 2$) scheme. Figure 4.1 shows the time evolution of the numerical solution, demonstrating the non-isotropic nature of this model.

A key property of the schemes derived in this paper is that they are designed, at the semi-discrete level, to either conserve or dissipate the energy. Figure 4.2 shows the time evolution of the discrete energy

$$E = \sum_{i,j=1}^{N} \int_{\Omega_{ij}} \frac{p^2 + \alpha v^2 + \beta w^2}{2} \, \mathrm{d}x = \frac{\Delta x \, \Delta y}{8} \sum_{i,j=1}^{N} \sum_{k,l=0}^{s} \rho_k \rho_l \left(\left(p_{ij}^{(kl)} \right)^2 + \alpha \left(v_{ij}^{(kl)} \right)^2 + \beta \left(w_{ij}^{(kl)} \right)^2 \right),$$

$$\tag{4.3}$$

for the Gaussian initial value problem using both conservative and dissipative schemes for $s \in \{0, \cdots, 3\}$. The results clearly indicate that the energy preserving (and dissipating) properties carry over to the fully discrete case when using a higher-order time integrator.

4.2. **Loss of regularity.** A crucial property for the 1D variational wave equation is that solutions loose regularity in finite time even for smooth initial data. For the 2D case this is still an open problem. We investigate this numerically by considering the initial value problem (1.6) with data

$$u_0(x, y) = \exp\left(-\left(x^2 + y^2\right)\right) \tag{4.4a}$$

$$u_1(x, y) = -c(u_0(x, y))u_{0,x}(x, y) \tag{4.4b}$$

for $(x, y) \in \mathbb{R}^2$. A numerical experiment was performed using $N = 64$ computational cells with the conservative and dissipative piecewise quadratic schemes. The results, shown in Figure 4.3, indicates a clear steepening of the gradient as the solution evolves.

Smooth solutions of (1.6) satisfies the conservation law (2.19). The root-mean-square of the residual (2.18) can therefore be an indicator function for loss of regularity in the solution. Figure 4.4 shows the residual at $t = 10$ for both the conservative and dissipative schemes. The results indicate that the solution looses smoothness near the front of the wave propagating in the positive x direction. Moreover, as expected, the dissipative scheme with the shock capturing operator is

(A) $t = 0$ (B) $t = 1/3$

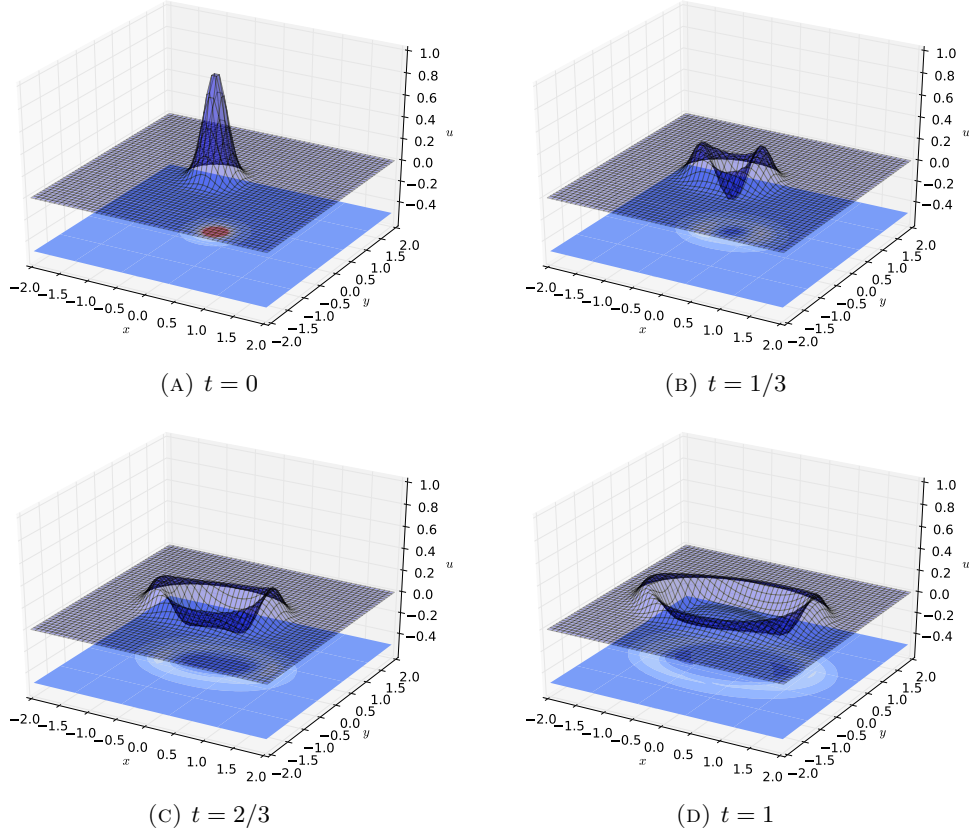(C) $t = 2/3$ (D) $t = 1$

FIGURE 4.1. Numerical solution of the initial value problem (1.6) with the initial data (4.2) using the dissipative piecewise quadratic scheme with $N = 32$. The parameters are $\alpha = 1.5$ and $\beta = 0.5$.
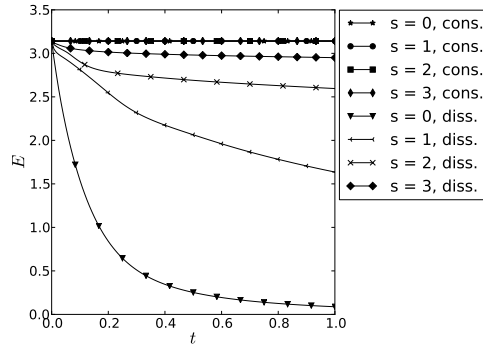

FIGURE 4.2. Evolution of the discrete energy (4.3) for the numerical solutions of the initial value problem (1.6) with the initial data (4.2) using both conservative and dissipative schemes. The parameters were $\alpha = 1.5$ and $\beta = 0.5$ and a $N = 32$ grid size was used.
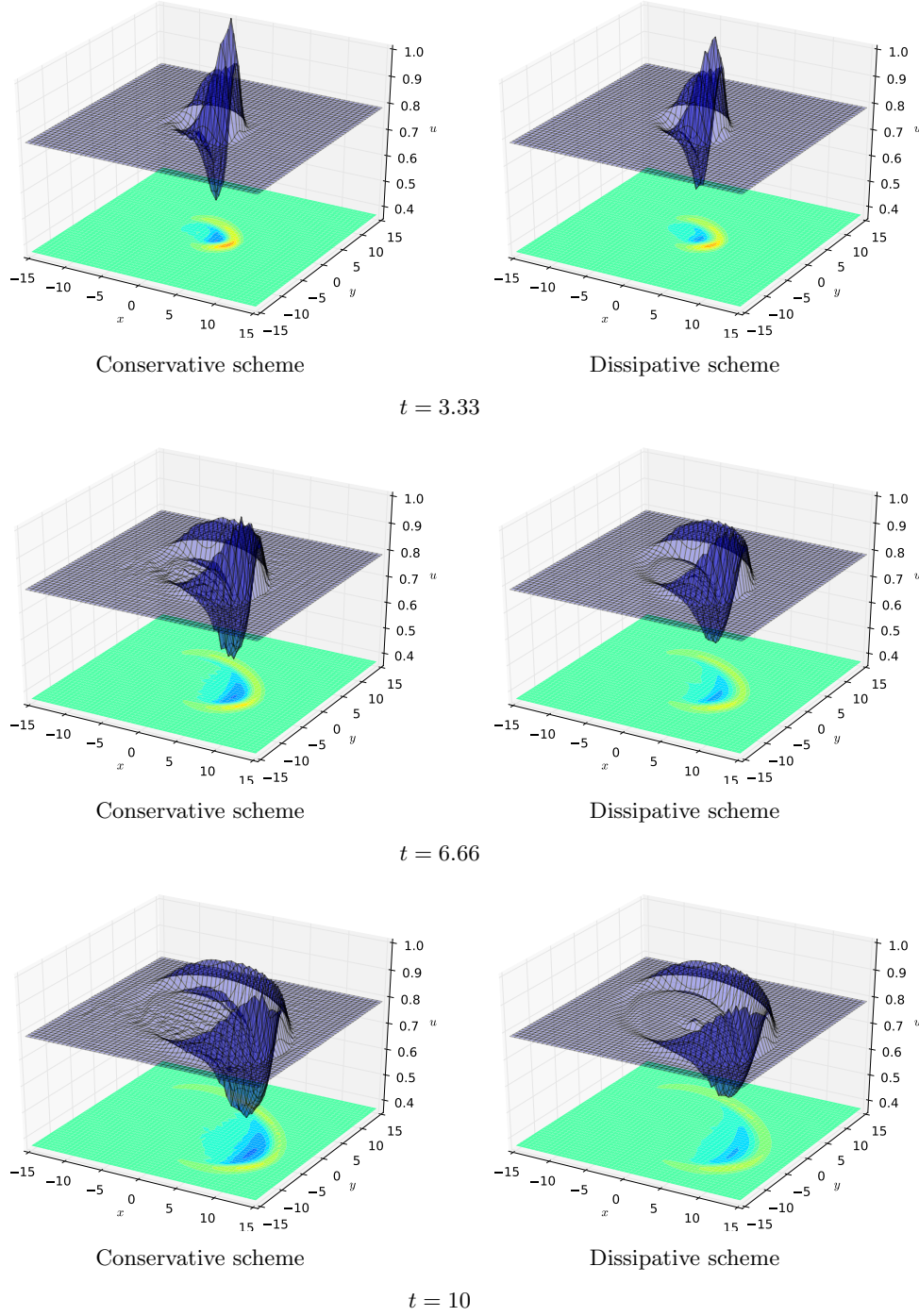
FIGURE 4.3. The numerical solution at for left) the piecewise quadratic conservative scheme and right) the piecewise quadratic dissipative scheme of the initial value problem (1.6) with initial data (4.4) with $N = 64$ cells. The physical parameters were $\alpha = 1.5$ and $\beta = 0.5$.

able to maintain a higher degree of numerical smoothness (as measured by the residual) than the conservative scheme.

(A) Conservative scheme   (B) Dissipative scheme
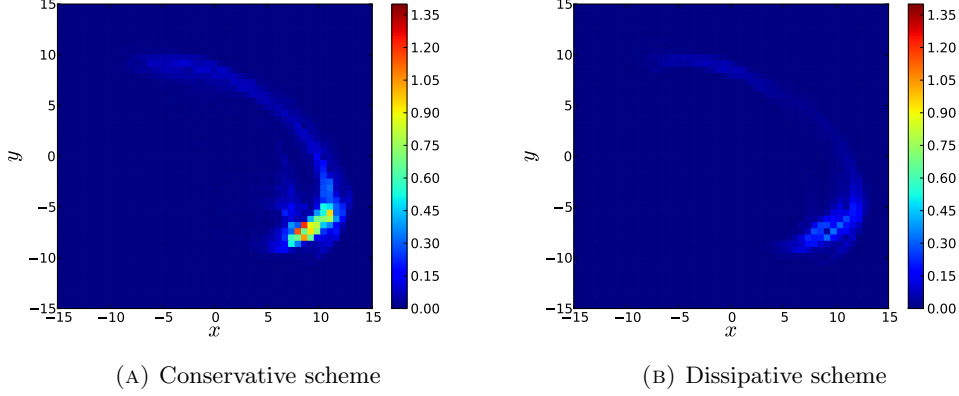
FIGURE 4.4. The root-mean-square of the residual (2.18) at $t = 10$ for the initial value problem (1.6) with initial data (4.4). At the left: the piecewise quadratic conservative scheme and at the right: the piecewise quadratic dissipative scheme, both with $N = 64$ cells. The physical parameters were $\alpha = 1.5$ and $\beta = 0.5$.

4.3. **Bifurcation of solutions.** Another critical feature of the 1D nonlinear variational wave equation (1.4) is the existence of different classes of weak solutions. However, the existence and well-posedness for the initial value problem in the 2D generalization remains an open problem.

In order to investigate this issue numerically, we consider the initial data 4.3 and study the convergence of the three schemes; the conservative DG scheme, the dissipative DG scheme and the Hamiltonian scheme; after the loss of regularity. Figure 4.5 shows the L^2 distance between the numerical solutions for different times and under grid refinement. The results indicate that the conservative DG scheme and the Hamiltonian scheme indeed converge to the same solution as the grid is refined. However, the distance between the dissipative and conservative DG schemes seems to converge to a non-zero value that increases as a function of time. This may indicate that the question of well-posedness for the 2D variational wave equation is as delicate as in the 1D case.
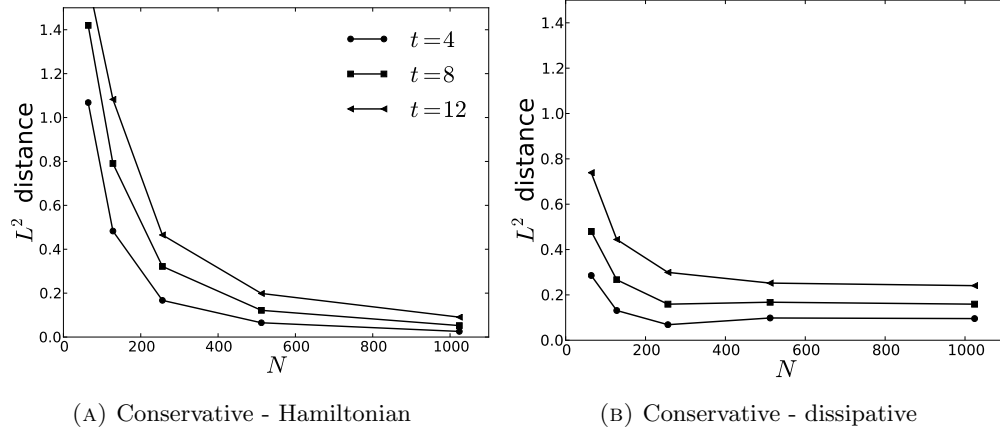

(A) Conservative - Hamiltonian   (B) Conservative - dissipative

FIGURE 4.5. The L^2 distance between left: the conservative DG scheme and the Hamiltonian scheme and right: the conservative DG scheme and the dissipative DG scheme, for the initial value problem (1.6) with initial data (4.4). The physical parameters were $\alpha = 1.5$ and $\beta = 0.5$.

4.4. **Order of Convergence and Efficiency.** In the following, we demonstrate the order of convergence and efficiency of both the conservative and dissipative schemes for smooth solutions. As before, we consider the initial value problem (1.6) with the initial data (4.2) with physical parameters $\alpha = 1.5$ and $\beta = 0.5$. A reference solution u_{ref} was calculated at $t = 0.1$ using the conservative piecewise cubic scheme ($s = 3$) with $N = 1024$. Figure 4.6 shows the error

$$e = \|u_N - u_{\text{ref}}\|_2 \tag{4.5}$$

for different grid cell numbers $N = N_x = N_y$. The results indicate a suboptimal order of conver-

(A) Conservative scheme

(B) Dissipative scheme

(C) Hamiltonian scheme
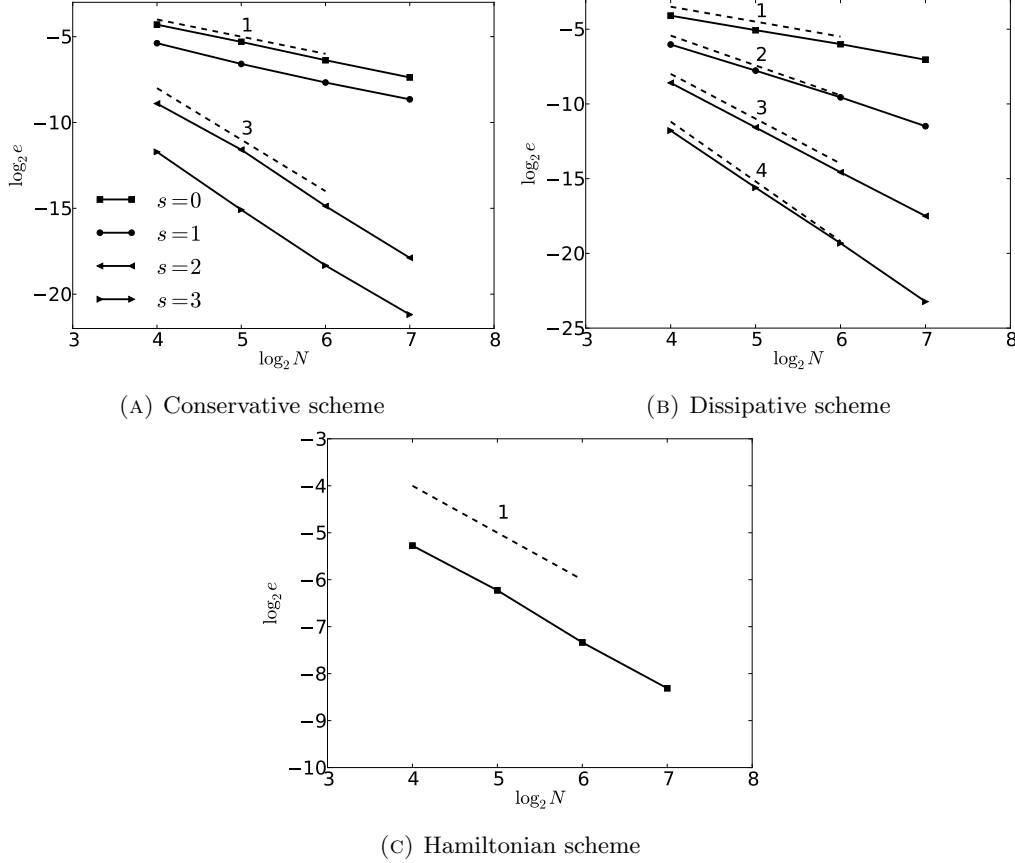
FIGURE 4.6. The error (4.5) for the numerical solution of the Gaussian initial value problem (4.2) as a function of N, using $\alpha = 1.5$ and $\beta = 0.5$. The dashed lines indicate the different orders of convergence.

gence for odd s when using the conservative numerical flux. For the dissipative scheme the order of convergence is optimal. This behavior has been observed also in the 1D case [1], and for certain DG schemes in the literature [24]. The Hamiltonian scheme converges to first order.

Figure 4.7 shows the error (4.5) compared to a a reference solution as a function of computational cost (CPU wall time). The results indicate that the higher-order schemes mostly make up for their increased computational complexity in better accuracy per CPU time. One exception is the conservative piecewise linear scheme, which for this case requires more computational work than the piecewise constant scheme in order to obtain the same accuracy. A possible explanation for this is that enforcing energy preservation using piecewise linear elements results in an un-physically jagged solution in certain regions. This happens despite the fact that the converged solution does not exhibit this behavior. For the piecewise linear dissipative scheme, this effect is suppressed by the added artificial viscosity.

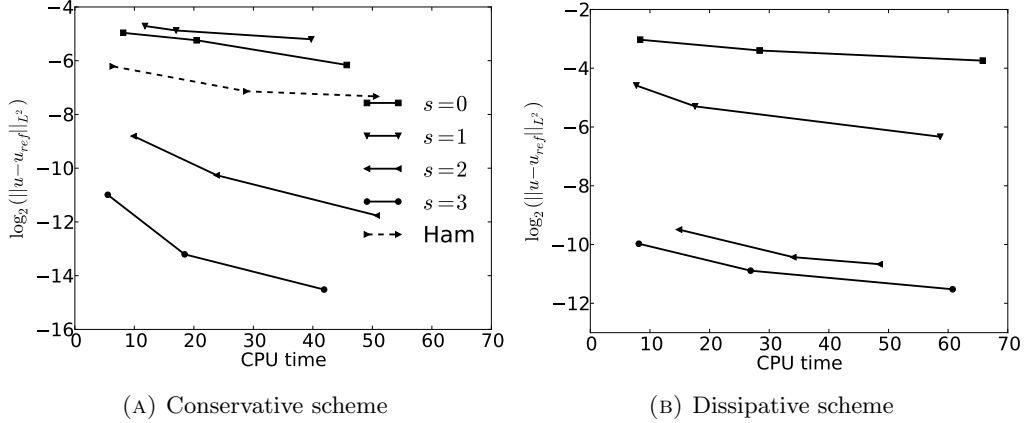(A) Conservative scheme   (B) Dissipative scheme

FIGURE 4.7. The error (4.5) for the numerical solution of the Gaussian initial value problem (4.2) at $t = 0.5$ as a function of CPU time (wall time), using $\alpha = 1.5$ and $\beta = 0.5$. The reference solution was calculated using the piecewise cubic conservative scheme with $N = 1024$ cells.

4.5. **Relaxation from a standing wave.** For this experiment we consider the initial value problem

$$u_0(x, y) = 2\cos(2\pi x)\sin(2\pi x) \tag{4.6a}$$

$$u_1(x, y) = \sin(2\pi(x - y)) \tag{4.6b}$$

on $(x, y) \in [0, 1] \times [0, 1]$ with periodic boundary conditions. The initial value problem can be seen as describing the following: Initially, a standing wave is induced in the director field using e.g. an external electromagnetic field or mechanical vibrations. At $t = 0$, the external influence is removed, and the evolution of the director is purely governed by elastic forces.
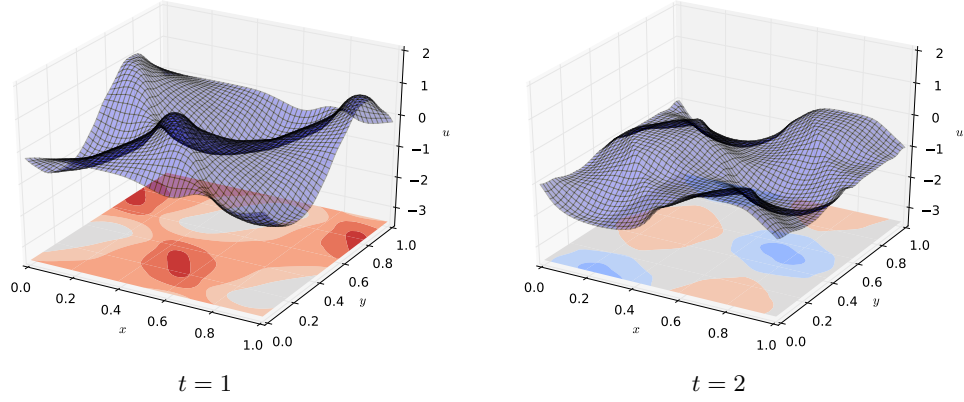
Figure 4.8 shows the numerical solution using both conservative and dissipative piecewise quadratic schemes with $N = 64$ cells. For comparison, a numerical solution was also computed using the Hamiltonian scheme derived in Section 3. The physical parameters were, as before, $\alpha = 1.5$ and $\beta = 0.5$. For $t > 0$ the non-isotropic elasticity of the director field deteriorates the initial standing wave and the pattern becomes more complicated. At $t = 2$ the solution given by the dissipative DG scheme is visibly more regular that the solutions given by the conservative schemes (DG and Hamiltonian).

5. SUMMARY

Using the Discontinuous Galerkin framework we have derived arbitrarily high-order numerical schemes for the 2D variational wave equation describing the director field in a type of nematic liquid crystals. By design, these schemes either conserve or dissipate the total mechanical energy of the system. The energy conserving scheme is based on a centralized numerical flux, while the dissipative scheme employs a dissipative flux combined with a shock capturing operator.

We have performed extensive numerical experiments both to verify the performance of the schemes and to investigate the behavior of solutions to the variational wave equation. In particular:

- The schemes converge to a high order of accuracy for smooth solutions.
- The high-order schemes outperform low-order scheme in terms of error per CPU time.
- The energy respecting properties (proven at the semi-discrete level) also hold on the fully discrete level when using a high-order numerical integration in time.
- Experiments show that the solution can loose regularity in finite time even for smooth initial data.
- After loss of regularity, results indicate that the conservative and dissipative schemes converge to different solutions as the grid is refined.
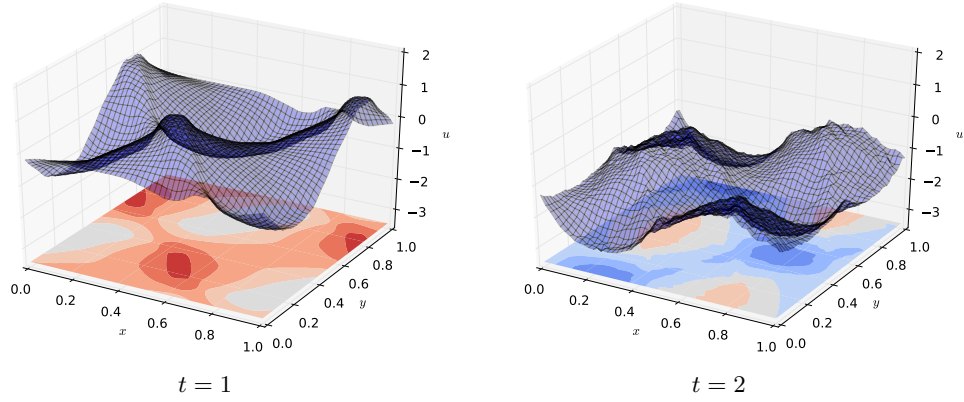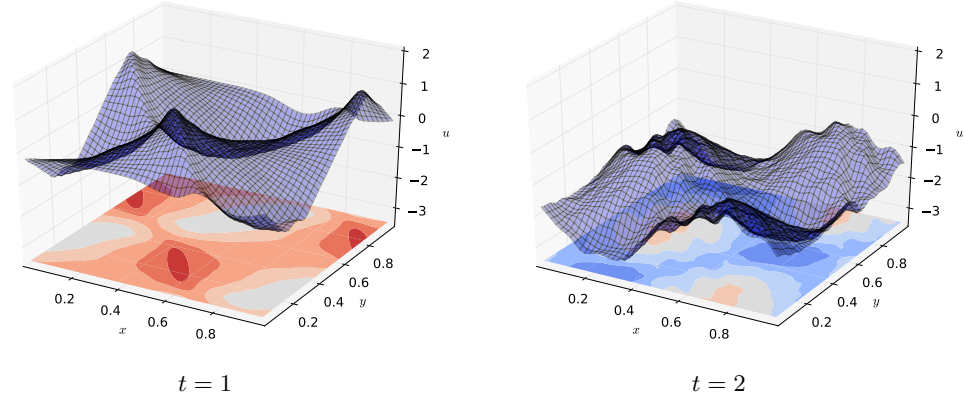
FIGURE 4.8. The numerical solution at left: $t = 1$ and right: $t = 2$ of the initial value problem (1.6) with initial data (4.6) using the conservative and dissipative piecewise quadratic schemes ($s = 3$) with $N = 64$ cells. The bottom row shows the numerical solution using the Hamiltonian scheme. The physical parameters were $\alpha = 1.5$ and $\beta = 0.5$.

To the best of our knowledge, this is the first systematic numerical study of the 2D generalization of the nonlinear variational wave equation (1.4). Indeed, the results here indicate that the mathematical treatment of (1.6) might be as delicate as in the 1D case.

References

[1] P. Aursand and U. Koley. Local discontinuous Galerkin schemes for a Nonlinear variational wave equation modeling liquid crystals, Preprint 2014

[2] T. J. Barth. Numerical methods for gas-dynamics systems on unstructured meshes. In: *An introduction to recent developments in theory and numerics of conservation laws Lecture notes in computational science and engineering*, vol(5), Springer, Berlin. Eds: D Kroner, M. Ohlberger, and C. Rohde, 1999.

[3] H. Berestycki, J. M. Coron and I. Ekeland. Variational Methods, Progress in nonlinear differential equations and their applications, *Vol 4*, Birkhäuser, Boston, 1990.

[4] A. Bressan and Y. Zheng. Conservative solutions to a nonlinear variational wave equation, *Commun. Math. Phys.*, 266: 471–497 (2006).

[5] G. Chavent and B. Cockburn. The local projection p^0p^1-discontinuous Galerkin finite element methods for scalar conservation law, *Math. Model. Numer. Anal.*, 23: 565–592 (1989).

[6] S. Y. Cockburn, B. Lin and C. W. Shu. TVB Runge-Kutta local projection discontinuous Galerkin finite element methods for conservation laws III: one dimensional systems, *J. Comput. Phys.*, 84: 90–113 (1989).

[7] J. Coron, J. Ghidaglia and F. Hélein. *Nematics*, Kluwer Academic Publishers, Dordrecht, 1991.

[8] J. L. Ericksen and D. Kinderlehrer. Theory and application of Liquid Crystals, *IMA Volumes in Mathematics and its Applications*, Vol 5, Springer Verlag, New York, 1987.

[9] X. Gang, S. Chang-Qing, and L. Lei Perturbed solutions in nematic liquid crystals under time-dependent shear. *Phys. Rew. A*, 36(1): 277–284 (1987).

[10] R. T. Glassey. Finite-time blow-up for solutions of nonlinear wave equations, *Math. Z.*, 177: 1761–1794 (1981).

[11] R. Glassey, J. Hunter, and Y. Zheng. Singularities and Oscillations in a nonlinear variational wave equation. In: J. Rauch and M. Taylor, editors, *Singularities and Oscillations*, Volume 91 of the IMA volumes in Mathematics and its Applications, pages 37–60. Springer, New York, 1997.

[12] R. T. Glassey, J. K. Hunter and Yuxi. Zheng. Singularities of a variational wave equation, *J. Diff. Eq.*, 129: 49–78 (1996).

[13] T. R. Hill and W. H. Reed. Triangular mesh methods for neutron transport equation, *Tech. Rep. LA-UR-73-479.*, Los Alamos Scientific Laboratory, 1973.

[14] A. Hiltebrand and S. Mishra. Entropy stable shock capturing space–time discontinuous Galerkin schemes for systems of conservation laws, *Numer. Math.* 126(1): 103–151 (2014).

[15] H. Holden and X. Raynaud. Global semigroup for the nonlinear variational wave equation, *Arch. Rat. Mech. Anal.*, 201(3): 871–964 (2011).

[16] H. Holden, K. H. Karlsen, and N. H. Risebro. A convergent finite-difference method for a nonlinear variational wave equation, *IMA. J. Numer. Anal.*, 29(3): 539–572 (2009).

[17] J. K. Hunter and R. A. Saxton. Dynamics of director fields, *SIAM J. Appl. Math.*, 51: 1498–1521 (1991).

[18] C. Johnson, P. Hansbo and A. Szepessy, On the convergence of shock capturing streamline diffusion methods for hyperbolic conservation laws, *Math. Comput.*, 54(189): 107–129 (1990).

[19] O. A. Kapustina. Liquid crystal acoustics: A modern view of the problem. *Crystallogr. Rep.* 49(4): 680–692 (2004)

[20] U. Koley, S. Mishra, N. H. Risebro, and F. Weber. Robust finite-difference schemes for a nonlinear variational wave equation modeling liquid crystals, *Submitted*.

[21] F. M. Leslie. Theory of flow phenomena in liquid crystals, *Liquid Crystals*, 4, 1–81 (1979).

[22] H. A. Luther and H. P. Konen. Some fifth-order classical Runge–Kutta formulas *SIAM Review*, 7(4): 551–558 (1965).

[23] R. A. Saxton. Dynamic instability of the liquid crystal director, *Contemporary Mathematics Vol 100*, Current Progress in Hyperbolic Systems, pages 325–330, ed. W. B. Lindquist, AMS, Providence, 1989.

[24] C.-W. Shu. Different formulations of the discontinuous Galerkin method for the viscous terms, In: *Conference in Honor of Professor H.-C. Huang on the occasion of his retirement*, Science Press, 14–45, 2000.

[25] I. W. Stewart. *The Static and Dynamic Continuum theory of liquid crystals: a mathematical introduction*, CRC Press, Boca Raton, 2004.

[26] C. Z. van Doorn. Dynamic behavior of twisted nematic liquidcrystal layers in switched fields. *J. Appl. Phys.*, 46: 3738–3745 (1975).

[27] V. A. Vladimirov and M. Y. Zhukov. Vibrational freedericksz transition in liquid crystals. *Phys. Rev. E*, 76:031706 (2007).

[28] C. K. Yun. Inertial coefficient of liquid crystals: A proposal for its measurements. *Phys. Lett. A*, 45(2): 119–120 (1973).

[29] P. Zhang and Y. Zheng. On oscillations of an asymptotic equation of a nonlinear variational wave equation, *Asymptot. Anal.*, 18(3): 307–327 (1998).

[30] P. Zhang and Y. Zheng. Singular and rarefactive solutions to a nonlinear variational wave equation, *Chin. Ann. Math.*, 22: 159–170 (2001).

[31] P. Zhang and Y. Zheng. Rarefactive solutions to a nonlinear variational wave equation of liquid crystals, *Commun. Partial Differ. Equ.*, 26: 381–419 (2001).

[32] P. Zhang and Y. Zheng. Weak solutions to a nonlinear variational wave equation, *Arch. Rat. Mech. Anal.*, 166: 303–319 (2003).

[33] P. Zhang and Y. Zheng. Weak solutions to a nonlinear variational wave equation with general data, *Ann. Inst. H. Poincaré Anal. Non Linéaire*, 22: 207–226 (2005).

[34] P. Zhang and Y. Zheng. On the global weak solutions to a nonlinear variational wave equation, *Handbook of Differential Equations. Evolutionary Equations*, ed. C. M. Dafermos and E. Feireisl, vol. 2, pages 561–648, Elsevier, 2006.

(Peder Aursand)
DEPARTMENT OF MATHEMATICAL SCIENCES,
NORWEGIAN UNIVERSITY OF SCIENCE AND TECHNOLOGY,
NO–7491 TRONDHEIM, NORWAY.
  E-mail address: `peder.aursand@math.ntnu.no`

(Ujjwal Koley)
TATA INSTITUTE OF FUNDAMENTAL RESEARCH,
CENTRE FOR APPLICABLE MATHEMATICS,
POST BAG NO. 6503, GKVK POST OFFICE,
SHARADA NAGAR, CHIKKABOMMASANDRA,
BANGALORE 560065, INDIA.
  E-mail address: `ujjwal@math.tifrbng.res.in`